Electronic Supplementary Material (ESI) for ChemComm.

Electronic Supplementary Information

Nitrous oxide activation by picoline-derived Ni-CNP hydrides

José Bermejo,[a] Isabel Ortega-Lepe,[a] Laura L. Santos,[a] Nuria Rendón,[a] Joaquín López-Serrano,[a] Eleuterio Álvarez[a] and Andrés Suárez*[a]

[a] Instituto de Investigaciones Químicas (IIQ), Departamento de Química Inorgánica, and Centro de Innovación en Química Avanzada (ORFEO-CINQA), CSIC-Universidad de Sevilla. Avda. Américo Vespucio 49, 41092, Sevilla, Spain.

E-mail: andres.suarez@iiq.csic.es

Table of Contents

1. Synthetic procedures and analytical data

1.1. General procedures

All reactions and manipulations were performed under nitrogen or argon, either in a Braun Labmaster 100 glovebox or using standard Schlenk-type techniques. All solvents were distilled under nitrogen with the following desiccants: sodium-benzophenone-ketyl for diethyl ether (Et_2O) and tetrahydrofuran (THF); sodium for toluene; CaH_2 for dichloromethane and acetonitrile (CH_2Cl_2, CH_3CN); and NaOMe for methanol (MeOH). All other reagents were purchased from commercial suppliers and used as received. NMR spectra were obtained on Bruker AVANCE NEO-300, AVANCE NEO-400, AVANCE III-400R and AVANCE NEO-500 spectrometers. $^{31}P\{^1H\}$ and $^{11}B\{^1H\}$ NMR shifts were referenced to external 85% H_3PO_4 and $BF_3{\cdot}Et_2O$, respectively, while $^{13}C\{^1H\}$ and ^1H shifts were referenced to the residual signals of deuterated solvents. All data are reported in ppm downfield from Me_4Si. All NMR measurements were carried out at 25 °C, unless otherwise stated. NMR signal assignations were confirmed by two dimensional (2D) NMR spectroscopy, including $^1H-^1H$ correlated spectroscopy (COSY), $^1H-^1H$ nuclear Overhauser effect spectroscopy (NOESY), $^1H-^{13}C$ heteronuclear single quantum coherence (HSQC), and $^1H-^{13}C$ heteronuclear multiple bond correlation (HMBC), for all of the complexes. HRMS data were obtained on a JEOL JMS-SX 102A mass spectrometer at the Instrumental Services of Universidad de Sevilla (CITIUS). Elemental analyses were run by the Analytical Service of the Instituto de Investigaciones Químicas in a Leco TrueSpec CHN elemental analyser. IR spectra were acquired on a Thermo Scientific Nicolet iS5 iD7 ATR instrument.

1.2. Synthesis and characterisation of imidazolium salts 1

Imidazolium salts **1a-b** were prepared following the synthetic methodology previously reported by Danopoulos, Braunstein *et al.*[1]

*Synthesis of the imidazolium salt **1a***

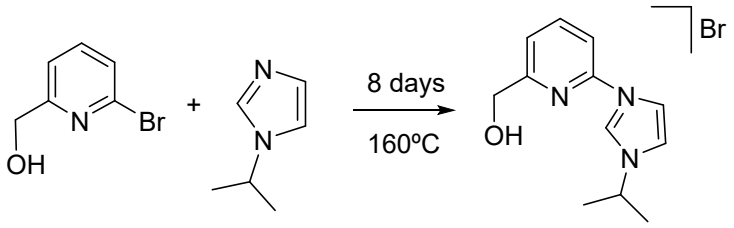

Aa

A mixture of 6-bromo-2-(hydroxymethyl)pyridine (1.50 g, 8.0 mmol) and 1-isopropyl-1*H*-imidazole (0.881 g, 8.0 mmol) was heated to 160 ºC for 8 days. The resulting solid was washed with Et_2O (3 x 20 mL). White solid (1.20 g, 50%).

^{1}H NMR (400 MHz, CD_3OD): δ 9.98 (dd, $^4J_{HH}$ = 1.6 Hz, $^4J_{HH}$ = 1.6 Hz, 1H, H arom Imid), 8.46 (br s, 1H, H arom Imid), 8.16 (dd, $^3J_{HH}$ = 8.4 Hz, $^3J_{HH}$ = 7.8 Hz, 1H, H arom Py), 8.01 (br s, 1H, H arom Imid), 7.86 (d, $^3J_{HH}$ = 8.4 Hz, 1H, H arom Py), 7.72 (d, $^3J_{HH}$ = 7.8 Hz, 1H, H arom Py), 4.86 (hept, $^3J_{HH}$ = 6.6 Hz, 1H, C*H*$(CH_3)_2$), 4.81 (s, 2H, CH_2O), 1.70 (d, $^3J_{HH}$ = 6.6 Hz, 6H, CH(C*H*$_3)_2$).

^{13}C{^{1}H} NMR (101 MHz, CD_3OD): δ 164.4 (C_q arom), 148.2 (C_q arom), 143.0 (CH arom), 139.4 (CH arom), 123.7 (CH arom), 123.6 (CH arom), 121.7 (CH arom), 113.9 (CH arom), 66.1 (CH_2O), 56.3 (*C*H$(CH_3)_2$), 23.7 (2 CH(*C*H$_3)_2$).

HRMS (ESI): *m/z* calcd for $C_{12}H_{16}N_3O$ [(*M*-Br)$^+$]: 218.1293; found: 218.1286.

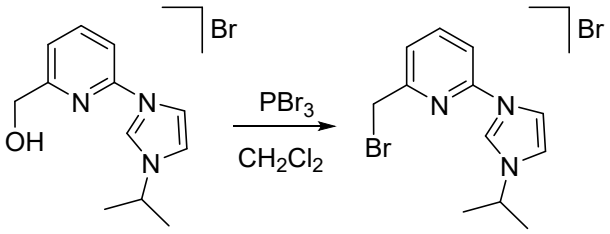

Aa **Ba**

To a solution of **Aa** (1.19 g, 4.0 mmol) in CH_2Cl_2 (30 mL) cooled to 0 ºC was added PBr_3 (0.38 mL, 4.0 mmol) dropwise. The resulting solution was stirred at room temperature for 24 h. The reaction mixture was treated with a saturated aqueous solution of Na_2CO_3

[1] T. Simler, A. A. Danopoulos and P. Braunstein, *Chem. Commun.,* 2015, **51**, 10699–10702.

until pH = 5-6. The aqueous phase was separated, and extracted with CH_2Cl_2 (4 x 20 mL). Organic phases were combined, and dried over Na_2SO_4. The desired product was obtained after evaporation of the solvent as a white solid (0.649 g, 45%).

^{1}H NMR (500 MHz, $CDCl_3$): δ 11.66 (dd, $^4J_{HH}$ = 1.2 Hz, $^4J_{HH}$ = 1.6 Hz, 1H, H arom Imid), 8.68 (d, $^3J_{HH}$ = 8.2 Hz, 1H, H arom Py), 8.37 (dd, $^2J_{HH}$ = 1.9 Hz, $^4J_{HH}$ = 1.6 Hz, 1H, H arom Imid), 8.02 (dd, $^3J_{HH}$ = 8.2 Hz, $^3J_{HH}$ = 8.2 Hz, 1H, H arom Py), 7.68 (dd, $^2J_{HH}$ = 1.9 Hz, $^4J_{HH}$ = 1.2 Hz, 1H, H arom Imid), 7.55 (d, $^3J_{HH}$ = 8.2 Hz, 1H, H arom Py), 5.17 (hept, 1H, $^3J_{HH}$ = 6.6 Hz, C*H*$(CH_3)_2$), 4.51 (s, 2H, CH_2Br), 1.72 (d, 6H, $^3J_{HH}$ = 6.6 Hz, CH(C*H*$_3)_2$).

^{13}C{^{1}H} NMR (126 MHz, $CDCl_3$): δ 157.0 (CH arom), 145.8 (C_q arom), 142.1 (CH arom), 135.2 (C_q arom), 125.0 (CH arom), 120.4 (CH arom), 119.4 (CH arom), 114.9 (CH arom), 54.6 (*C*H$(CH_3)_2$), 32.3 (CH_2Br), 23.5 (CH(*C*H$_3)_2$).

HRMS (ESI): *m/z* calcd for $C_{12}H_{15}BrN_3$ [(*M*-Br)$^+$]: 280.0449; found: 280.0446.

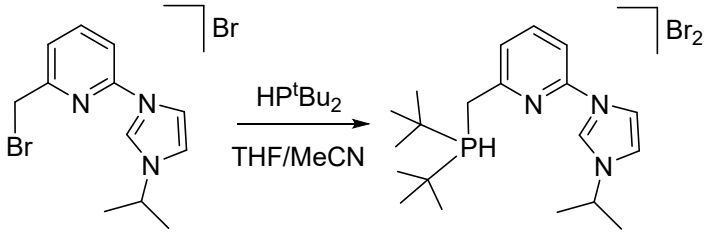

Ba **1a**

To a solution of **Ba** (0.326 g, 0.90 mmol) in THF (3 mL) / MeCN (9 mL) was added HP^{t}Bu$_2$ (0.25 mL, 1.4 mmol) dropwise. The resulting solution was stirred at room temperature for 3 days. Volatiles were removed under vacuum, and the resulting solid was washed with cold THF (2 x 5 mL) to give a yellow solid (0.308 g, 67%).

^{1}H NMR (400 MHz, CD_2Cl_2): δ 11.65 (s, 1H, H arom Imid), 9.54 (dt, $^1J_{HP}$ = 504 Hz, $^3J_{HH}$ = 5.1 Hz, 1H, ^{t}Bu$_2$P*H*), 8.99 (s, 1H, H arom Imid), 8.34 (d, $^3J_{HH}$ = 8.0 Hz, 1H, H arom Py), 8.15 (d, $^3J_{HH}$ = 7.4 Hz, 1H, H arom Py), 8.05 (dd, $^3J_{HH}$ = 8.04, $^3J_{HH}$ = 7.4 Hz, 1H, H arom Py), 7.68 (s, 1H, H arom imid), 5.41 (hept, $^3J_{HH}$ = 6.7 Hz, 1H, C*H*$(CH_3)_2$), 4.42 (dd, $^2J_{HP}$ = 13.1 Hz, $^3J_{HH}$ = 5.1 Hz, 2H, C*H*$_2$P), 1.72 (d, $^3J_{HH}$ = 6.7 Hz, 6H, 2 CH(C*H*$_3)_2$), 1.62 (d, $^3J_{HP}$ = 16.4 Hz, 18H, 2 C(C*H*$_3)_3$).

^{13}C{^{1}H} NMR (101 MHz, CD_2Cl_2): δ 153.7 (d, J_{CP} = 11 Hz, C_q arom), 146.9 (C_q arom), 142.8 (CH arom), 135.9 (CH arom), 127.2 (d, J_{CP} = 7 Hz, CH arom), 121.4 (CH arom), 121.1 (CH arom), 114.6 (CH arom), 54.6 (*C*H$(CH_3)_2$), 33.9 (d, J_{CP} = 37 Hz, 2 *C*$(CH_3)_3$), 28.2 (6 C(*C*H$_3)_3$), 24.7 (d, J_{CP} = 42 Hz, C*H*$_2$P), 23.6 (2 CH(*C*H$_3)_2$).

$^{31}P\{^{1}H\}$ NMR (162 MHz, CD_2Cl_2): δ 28.3 ppm.

HRMS (ESI): *m/z* calcd for $C_{20}H_{33}N_3P$ [(*M*-HBr-Br)$^+$]: 346.2490; found: 346.2404.

*Synthesis of the imidazolium salt **1b***

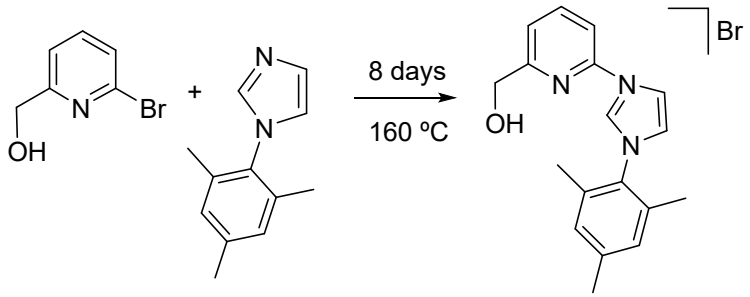

Ab

A mixture of 6-bromo-2-(hydroxymethyl)pyridine (1.49 g, 8.0 mmol) and 1-mesityl-1*H*--imidazole (1.50 g, 8.0 mmol) was heated to 160 ºC for 8 days. The resulting solid was washed with Et_2O (3 x 20 mL), and crystallized from a CH_2Cl_2/toluene solvent mixture. White solid (1.161 g, 39%).

^{1}H NMR (400 MHz, CD_3OD): δ 10.22 (s, 1H, H arom Imid), 8.72 (d, $^{3}J_{HH}$ = 2.0 Hz, 1H, H arom Imid), 8.18 (dd, $^{3}J_{HH}$ = 8.0 Hz, $^{3}J_{HH}$ = 8.0 Hz, 1H, H arom Py), 7.98 (d, $^{3}J_{HH}$ = 2.0 Hz, 1H, H arom Imid), 7.97 (d, $^{3}J_{HH}$ = 8.0 Hz, 1H, H arom Py), 7.77 (d, $^{3}J_{HH}$ = 8.0 Hz, 1H, H arom Py), 7.21 (s, 2H, 2 H arom Mes), 4.83 (s, 2H, CH_2O), 2.42 (s, 3H, CH_3 Mes), 2.21 (s, 6H, 2 CH_3 Mes).

$^{13}C\{^{1}H\}$ NMR (101 MHz, CD_3OD): δ 164.6 (C_q arom), 148.0 (C_q arom), 143.7 (C_q arom), 143.1 (CH arom), 136.6 (2 C_q arom), 133.3 (C_q arom), 131.7 (2 CH arom), 127.3 (CH arom), 127.2 (CH arom), 124.0 (CH arom), 122.3 (CH arom), 114.4 (CH arom), 66.1 (CH_2O), 22.0 (CH_3 Mes), 18.3 (2 CH_3 Mes).

HRMS (ESI): *m/z* calcd for $C_{18}H_{20}N_3O$ [(*M*-Br)$^+$]: 294.1606; found: 294.1604.

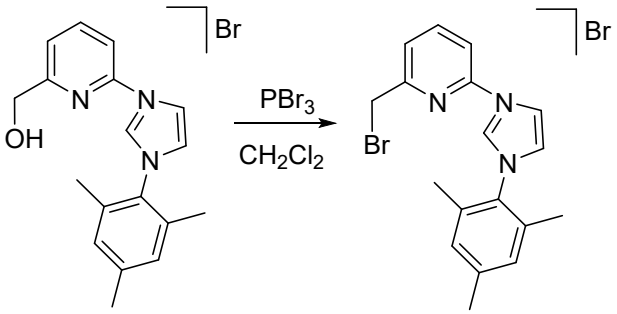

Ab **Bb**

To a solution of **Ab** (1.10 g, 3.0 mmol) in CH_2Cl_2 (30 mL) cooled to 0 ºC was added PBr_3 (0.28 mL, 3.0 mmol) dropwise. The resulting solution was stirred at room temperature for 24 h. The reaction mixture was treated with a saturated aqueous solution of Na_2CO_3 until pH = 5-6. The aqueous phase was separated, and extracted with CH_2Cl_2 (4 x 20 mL). Organic phases were combined, and dried over Na_2SO_4. The desired product was obtained after evaporation of the solvent as a white solid (1.02 g, 78%).

^{1}H NMR (400 MHz, CD_3OD): δ 10.20 (s, 1H, H arom Imid), 8.72 (d, $^3J_{HH}$ = 1.6 Hz, 1H, H arom Imid), 8.22 (dd, $^3J_{HH}$ = 8.0 Hz, $^3J_{HH}$ = 8.0 Hz, 1H, H arom Py), 8.01 (m, 2H, H arom Imid + H arom Py), 7.82 (d, $^3J_{HH}$ = 8.0 Hz, 1H, H arom Py), 7.21 (s, 2H, 2 H arom Mes), 4.74 (s, 2H, CH_2Br), 2.42 (s, 3H, CH_3 Mes), 2.21 (s, 6H, 2 CH_3 Mes).

^{13}C{^{1}H} NMR (101 MHz, CD_3OD): δ 160.1 (C_q arom), 148.4 (C_q arom), 143.7 (2 CH arom), 138.3 (C_q arom), 136.6 (2 C_q arom), 133.3 (C_q arom), 131.7 (2 CH arom), 127.4 (CH arom), 127.2 (CH arom), 122.4 (CH arom), 115.7 (CH arom), 33.6 (CH_2Br), 22.0 (CH_3 Mes), 18.3 (2 CH_3 Mes).

HRMS (ESI): *m/z* calcd for $C_{18}H_{20}BrN_3$ [(*M*-Br)$^+$]: 356.0762; found: 356.0760.

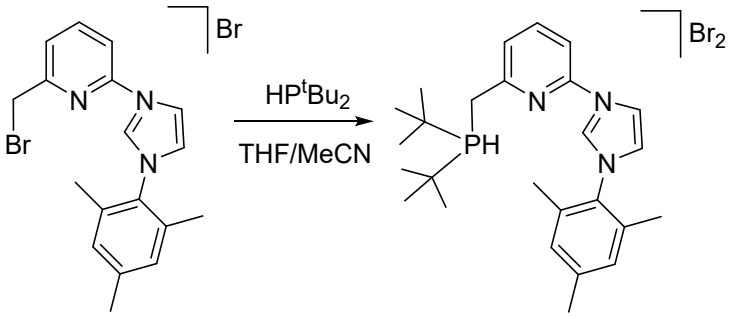

Bb **1b**

To a solution of **Bb** (0.673 g, 1.5 mmol) in THF (3 mL) / MeCN (9 mL) was added HP^tBu_2 (0.42 mL, 2.3 mmol) dropwise. The resulting solution was stirred at room temperature for

3 days. Volatiles were removed under vacuum, and the resulting solid was washed with cold THF (2 x 5 mL) to give a yellow solid (0.470 g, 53%).

^{1}H NMR (400 MHz, CD_2Cl_2): δ 11.53 (s, 1H, H arom Imid), 9.34 (dt, $^{1}J_{HP}$ = 500 Hz, $^{3}J_{HH}$ = 4.8 Hz, 1H, $^{t}Bu_2PH$), 9.55 (s, 1H, H arom Imid), 8.67 (d, $^{3}J_{HH}$ = 8.0 Hz, 1H, H arom Py), 8.25 (d, $^{3}J_{HH}$ = 8.0 Hz, 1H, H arom Py), 8.00 (dd, $^{3}J_{HH}$ = 8.0 Hz, $^{3}J_{HH}$ = 8.0 Hz, 1H, H arom Py), 7.53 (s, 1H, H arom Imid), 7.06 (s, 2H, 2 H arom Mes), 4.50 (dd, $^{2}J_{HP}$ = 13.0 Hz, $^{3}J_{HH}$ = 4.8 Hz, 2H, CH_2P), 2.34 (s, 3H, CH_3 Mes), 2.18 (s, 6H, 2 CH_3 Mes), 1.55 (d, $^{3}J_{HP}$ = 16.0 Hz, 18H, 2 $C(CH_3)_3$).

^{13}C{^{1}H} NMR (101 MHz, CD_2Cl_2): δ 152.9 (C_q arom), 146.3 (C_q arom), 142.1 (CH arom), 141.4 (C_q arom), 137.1 (C_q arom), 134.3 (2 C_q arom), 129.8 (CH arom), 129.7 (2 CH arom), 126.7 (CH arom), 124.4 (CH arom), 121.7 (CH arom), 115.1 (CH arom), 33.2 (d, J_{CP} = 34 Hz, 2 $C(CH_3)_3$), 27.4 (2 $C(CH_3)_3$), 23.9 (d, J_{CP} = 41 Hz, CH_2P), 20.9 (CH_3 Mes), 17.7 (2 CH_3 Mes).

^{31}P{^{1}H} NMR (162 MHz, CD_2Cl_2): δ 29.8 ppm.

HRMS (ESI): *m/z* calcd for $C_{26}H_{37}N_3P$ [(*M*-HBr-Br)$^{+}$]: 422.2725; found: 422.2722.

1.3. Synthesis and characterisation of nickel complexes 2

*Complex **2a***

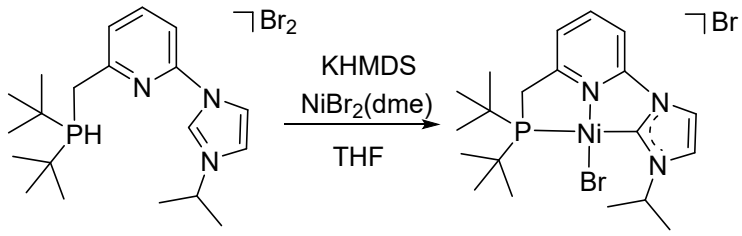

1a **2a**

KHMDS (0.079 g, 0.39 mmol) was added to a solution of **1a** (0.100 g, 0.20 mmol) in THF (10 mL), and the resulting mixture was stirred for 30 min. Then, $NiBr_2$(dme) (0.061 g, 0.20 mmol) was added, and the suspension was stirred overnight. Volatiles were removed under vacuum, and the residue was extracted with CH_2Cl_2 (2 × 10 mL). Solvent was evaporated, and the solid was washed with Et_2O (2 × 10 mL). Red solid (0.092 g, 83%).

^{1}H NMR (400 MHz, CD_2Cl_2): δ 8.76 (d, $^{3}J_{HH}$ = 1.3 Hz, 1H, H arom NHC), 8.50 (d, $^{3}J_{HH}$ = 8.1 Hz, 1H, H arom Py), 8.20 (dd, $^{3}J_{HH}$ = 8.1 Hz, $^{3}J_{HH}$ = 8.1 Hz, 1H, H arom Py), 7.57 (d, $^{3}J_{HH}$ = 8.1 Hz, 1H, H arom Py), 7.23 (d, $^{3}J_{HH}$ = 1.3 Hz, 1H, H arom NHC), 5.97 (m, 1H, C*H*$(CH_3)_2$), 3.56 (d, $^{2}J_{HP}$ = 9.8 Hz, 2H, CH_2P), 1.58 (d, $^{3}J_{HP}$ = 14.2 Hz, 18H, 2 C(C*H*$_3)_3$), 1.46 (d, $^{3}J_{HH}$ = 6.7 Hz, 6 H, CH(C*H*$_3)_2$).

^{13}C{^{1}H} NMR (101 MHz, CD_2Cl_2): δ 164.4 (d, J_{CP} = 8 Hz, C_q arom), 161.7 (d, J_{CP} = 102 Hz, C-2 NHC), 152.5 (C_q arom), 144.6 (CH arom), 122.1 (d, J_{CP} = 9 Hz, CH arom), 121.4 (CH arom), 119.0 (CH arom), 112.3 (CH arom), 51.4 (*C*H$(CH_3)_2$), 37.1 (d, J_{CP} = 15 Hz, 2 *C*$(CH_3)_3$), 34.9 (d, J_{CP} = 20 Hz, CH_2P), 29.8 (6 C(*C*H$_3)_3$), 23.7 (2 CH(*C*H$_3)_2$).

^{31}P{^{1}H} NMR (162 MHz, THF-d_8): δ 57.0 ppm.

Anal. Calcd (%) for $C_{20}H_{32}Br_2N_3NiP$: C 42.59, H 5.72, N 7.45; found C 42.18, H 5.79, N 7.77.

*Complex **2b***

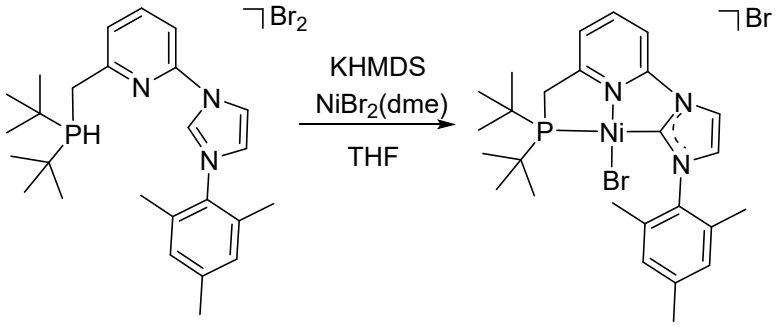

1b **2b**

KHMDS (0.144 g, 0.72 mmol) was added to a solution of **1b** (0.200 g, 0.34 mmol) in THF (15 mL), and the resulting mixture was stirred for 30 min. Then, $NiBr_2$(dme) (0.106 g, 0.34 mmol) was added, and the suspension was stirred overnight. Volatiles were removed under vacuum, and the residue was extracted with CH_2Cl_2 (2 × 10 mL). Solvent was evaporated and the solid was washed with Et_2O (2 × 10 mL). Orange solid (0.191 g, 87%).

^{1}H NMR (400 MHz, CD_2Cl_2): δ 9.27 (s, 1H, H arom NHC), 8.90 (d, $^{3}J_{HH}$ = 8.2 Hz, 1H, H arom Py), 8.29 (dd, $^{3}J_{HH}$ = 8.2 Hz, $^{3}J_{HH}$ = 8.2 Hz, 1H, H arom Py), 7.66 (d, $^{3}J_{HH}$ = 8.2 Hz, 1H, H arom Py), 7.00 (s, 2H, H arom Mes), 6.99 (s, 1H, H arom NHC), 3.65 (d, $^{2}J_{HP}$ = 9.6 Hz, 2H, CH_2P), 2.37 (s, 3H, CH_3 Mes), 2.16 (s, 6H, 2 CH_3 Mes), 1.53 (d, $^{3}J_{HP}$ = 14.5 Hz, 18H, 2 C(C*H*$_3)_3$).

$^{13}C\{^1H\}$ NMR (101 MHz, CD_2Cl_2): δ 164.5 (d, J_{CP} = 8 Hz, C_q arom), 164.4 (d, J_{CP} = 109 Hz, C-2 NHC), 152.6 (C_q arom), 144.6 (CH arom), 140.4 (C_q arom), 135.5 (C_q arom), 135.1 (2 C_q arom), 129.6 (2 CH arom), 127.0 (d, J_{CP} = 4 Hz, CH arom), 122.4 (d, J_{CP} = 8 Hz, CH arom), 119.7 (CH arom), 112.9 (CH arom), 36.8 (d, J_{CP} = 15 Hz, 2 $C(CH_3)_3$), 34.7 (d, J_{CP} = 20 Hz, CH_2P), 29.7 (2 $C(CH_3)_3$), 21.6 (CH_3 Mes), 18.5 (2 CH_3 Mes).

$^{31}P\{^1H\}$ NMR (162 MHz, CD_3CN): δ 57.8 ppm.

Anal. Calcd (%) for $C_{26}H_{36}Br_2N_3NiP$: C 48.79, H 5.67, N 6.57; found C 48.81, H 6.02, N 6.57.

1.4. Synthesis and characterisation of nickel complexes 3

*Complex **3a***

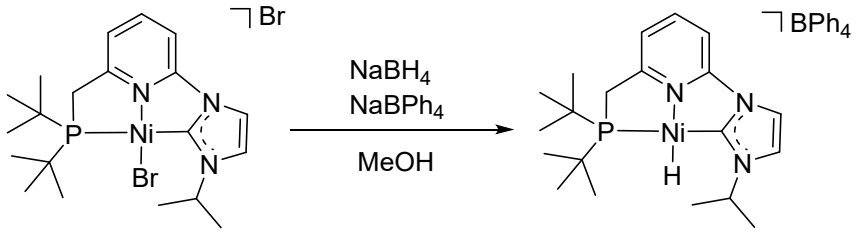

2a **3a**

Complex **2a** (0.050 g, 0.09 mmol) was dissolved in MeOH (7 mL), and $NaBH_4$ (0.017 g, 0.44 mmol) was added in two portions. When bubbling ended, a solution of $NaBPh_4$ (0.036 g, 0.11 mmol) in MeOH (1 mL) was added. The reaction mixture was left at room temperature for 2 h, and then cooled to -30 ºC for 3 days. After this time, red crystals were separated by filtration, and washed with Et_2O (4 × 3 mL). Red crystals (0.038 g, 68%).

^1H NMR (400 MHz, THF-d_8): δ 7.65 (dd, $^3J_{HH}$ = 8.0 Hz, $^3J_{HH}$ = 8.0 Hz, 1H, H arom Py), 7.39 (s, 1H, H arom NHC), 7.36 (m, 8H, H arom BPh_4), 7.27 (s, 1H, H arom NHC), 7.16 (d, $^3J_{HH}$ = 8.0 Hz, 1H, H arom Py), 7.04 (d, $^3J_{HH}$ = 8.0 Hz, 1H, H arom Py), 6.89 (dd, 8H, $^3J_{HH}$ = 7.0 Hz, H arom BPh_4) 6.74 (t, 4H, $^3J_{HH}$ = 7.0 Hz, H arom BPh_4) 4.91 (hept, $^3J_{HH}$ = 6.7 Hz, 1H, $CH(CH_3)_2$), 3.57 (d, $^2J_{HP}$ = 8.6 Hz, 2H, CH_2P), 1.50 (d, $^3J_{HH}$ = 6.7 Hz, 6H, $CH(CH_3)_2$), 1.38 (d, $^3J_{HP}$ = 14.4 Hz, 18H, 2 $C(CH_3)_3$), -18.00 (d, $^2J_{HP}$ = 71.8 Hz, 1H, NiH).

$^{13}C\{^1H\}$ NMR (101 MHz, THF-d_8): δ 178.8 (d, J_{CP} = 81 Hz, C-2 NHC), 166.6 (C_q arom), 166.1 (C_q arom), 165.6 (C_q arom), 165.1 (C_q arom), 163.7 (d, J_{CP} = 8 Hz, C_q arom), 152.3 (d, J_{CP} = 4 Hz, C_q arom), 143.9 (CH arom), 137.8 (8 CH arom BPh_4), 126.5 (8 CH arom BPh_4), 122.9 (d, J_{CP} = 8 Hz, CH arom), 122.6 (4 CH arom BPh_4), 120.8 (CH arom), 118.3 (CH arom) 109.7 (CH arom), 56.2 ($CH(CH_3)_2$), 35.5 (d, J_{CP} = 18 Hz, CH_2P), 35.3 (d, J_{CP} = 19 Hz, 2 $C(CH_3)_3$), 29.9 (d, J_{CP} = 5 Hz, 2 $C(CH_3)_3$), 23.8 (2 $CH(CH_3)_2$).

$^{31}P\{^1H\}$ NMR (162 MHz, THF-d_8): δ 85.8 ppm.

IR (ATR): 1901 cm^{-1} (m, ν_{NiH}).

Anal. Calcd (%) for $C_{44}H_{53}BN_3NiP$: C 72.95, H 7.37, N 5.80; found C 72.75, H 7.72, N 6.14.

*Complex **3b***

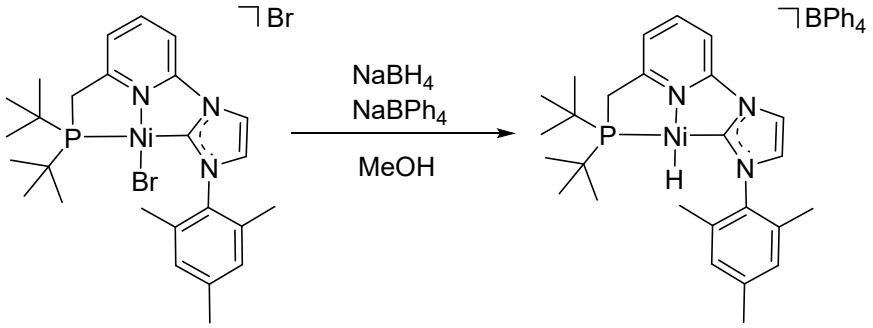

2b **3b**

Complex **2b** (0.050 g, 0.08 mmol) was dissolved in MeOH (7 mL), and $NaBH_4$ (0.015 mg, 0.39 mmol) was added in two portions. When bubbling ended, a solution of $NaBPh_4$ (0.032 g, 0.09 mmol) in MeOH (1 mL) was added. The reaction mixture was left at room temperature for 2 h, and then cooled to -30 ºC for 3 days. After this time, the precipitate was separated by filtration, and washed with Et_2O (4 × 3 mL). Yellow solid (0.046 g, 74%).

^1H NMR (400 MHz, THF-d_8): δ 7.67 (dd, $^3J_{HH}$ = 7.6 Hz, $^3J_{HH}$ = 7.6 Hz, 1H, H arom Py), 7.57 (s, 1H, H arom NHC), 7.36 (br s, 8H, H arom BPh_4), 7.19 (s, 1H, H arom NHC), 7.18 (br s, 1H, H arom Py), 7.07 (br s, 3H, H arom Py + 2 H arom Mes), 6.88 (dd, $^3J_{HH}$ = 7.6 Hz, 8H, H arom BPh_4) 6.73 (t, $^3J_{HH}$ = 7.0 Hz, 4H, H arom BPh_4), 3.56 (d, $^2J_{HP}$ = 8.7 Hz, 2 H, CH_2P), 2.38 (s, 3H, CH_3 Mes), 2.14 (s, 6H, 2 CH_3 Mes), 1.30 (d, $^3J_{HP}$ = 14.4 Hz, 18H, 2 $C(CH_3)_3$), -18.35 (d, $^2J_{HP}$ = 68.3 Hz, 1H, NiH).

$^{13}C\{^1H\}$ NMR (101 MHz, THF-d_8): δ 181.8 (d, J_{CP} = 83 Hz, C-2 NHC), 166.6 (C_q arom), 166.1 (C_q arom), 165.6 (C_q arom), 165.1 (C_q arom), 163.7 (d, J_{CP} = 8 Hz, C_q arom), 152.3 (d, J_{CP} = 4 Hz, C_q arom), 143.9 (CH arom), 140.6 (C_q arom), 137.8 (8 CH arom BPh_4), 137.6 (C_q arom), 135.6 (2 C_q arom), 130.5 (2 CH arom), 126.5 (8 CH arom BPh_4), 126.3 (CH arom), 123.2 (d, J_{CP} = 10 Hz, CH arom), 122.6 (4 CH arom BPh_4), 118.4 (CH arom), 110.2 (CH arom), 35.6 (d, J_{CP} = 21 Hz, CH_2P), 35.2 (d, J_{CP} = 18 Hz, 2 $C(CH_3)_3$), 29.9 (d, J_{CP} = 5 Hz, 2 $C(CH_3)_3$), 21.8 (CH_3 Mes), 18.8 (2 CH_3 Mes).

$^{31}P\{^1H\}$ NMR (162 MHz, CD_3CN): δ 85.2 ppm.

IR (ATR): 1888 cm^{-1} (m, ν_{NiH}).

Anal. Calcd (%) for $C_{50}H_{57}BN_3NiP$: C 75.02, H 7.18, N 5.25; found C 75.38, H 7.23, N 5.55.

1.5. Synthesis and characterisation of nickel complexes 4

*Complex **4a***

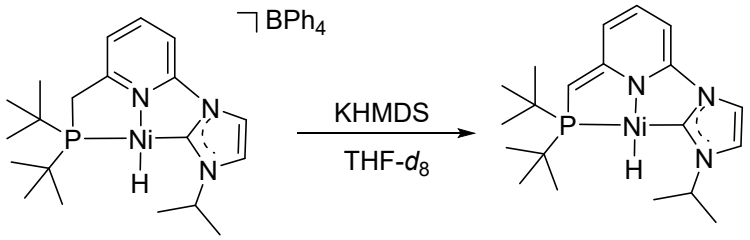

3a **4a**

In a J. Young-valved NMR tube, a solution of complex **3a** (0.015 g, 0.02 mmol) in THF-d_8 (0.45 mL) was treated with KHMDS (0.005 g, 0.03 mmol). The sample was analysed by NMR spectroscopy after 30 min, observing the formation of complex **4a**. The attempted isolation of the product was unsuccessful, and therefore was characterised spectroscopically.

^1H NMR (400 MHz, THF-d_8): δ 7.41 (s, 1H, H arom NHC), 7.20 (s, 1H, H arom NHC), 6.41 (dd, $^3J_{HH}$ = 9.2 Hz, $^3J_{HH}$ = 6.5 Hz, 1H, H arom Py), 5.95 (d, $^3J_{HH}$ = 9.2 Hz, 1H, H arom Py), 5.34 (d, $^3J_{HH}$ = 6.5 Hz, 1H, H arom Py), 5.00 (hept, 1H, $^3J_{HH}$ = 6.9 Hz, $CH(CH_3)_2$), 3.26 (s, 1H, CHP), 1.47 (d, 6H, $^3J_{HH}$ = 6.9 Hz, $CH(CH_3)_2$), 1.34 (d, $^3J_{HP}$ = 13.1 Hz, 18H, 2 $C(CH_3)_3$), -17.49 (d, 1H, $^2J_{HP}$ = 67.2 Hz, NiH).

$^{13}C\{^1H\}$ NMR (101 MHz, THF-d_8): δ 182.5 (d, J_{CP} = 73 Hz, C-2 NHC), 169.5 (d, J_{CP} = 19 Hz, C_q arom), 152.1 (C_q arom), 134.2 (CH arom), 117.9 (CH arom), 116.1 (CH arom), 113.6 (d, J_{CP} = 14 Hz, CH arom), 84.1 (CH arom), 65.1 (d, J_{CP} = 50 Hz, CHP), 54.9 (CH(CH_3)$_2$), 35.5 (d, J_{CP} = 24 Hz, 2 C(CH_3)$_3$), 30.5 (d, J_{CP} = 5 Hz, 2 C(CH_3)$_3$), 23.9 (2 CH(CH_3)$_2$).

$^{31}P\{^1H\}$ NMR (162 MHz, THF-d_8): δ 76.6 ppm.

IR (ATR): 1841 cm^{-1} (m, ν_{NiH}).

*Complex **4b***

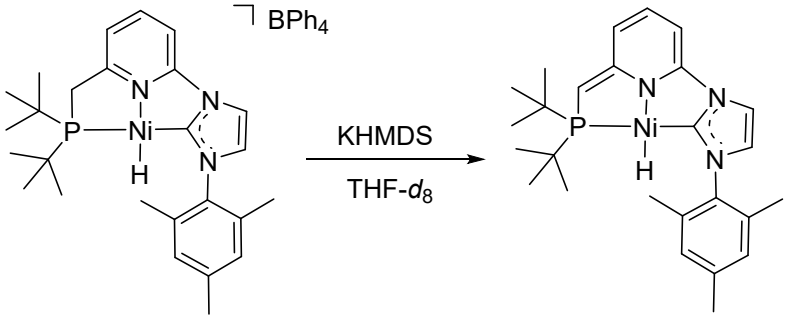

3b **4b**

In a J. Young-valved NMR tube, a solution of complex **3b** (0.015 g, 0.02 mmol) in THF-d_8 (0.45 mL) was treated with KHMDS (0.005 g, 0.02 mmol). The sample was analysed by NMR spectroscopy after 30 min, observing the formation of complex **4b**. The attempted isolation of the product was unsuccessful, and therefore was characterised spectroscopically.

^1H NMR (400 MHz, THF-d_8): δ 7.60 (s, 1H, H arom NHC), 7.07 (s, 1H, H arom NHC), 6.99 (s, 2 H, H arom Mes), 6.46 (dd, $^3J_{HH}$ = 8.8 Hz, $^3J_{HH}$ = 6.6 Hz, 1H, H arom Py), 5.99 (d, $^3J_{HH}$ = 8.8 Hz, 1H, H arom Py), 5.43 (d, $^3J_{HH}$ = 6.6 Hz, 1H, H arom Py), 3.27 (s, 1H, CHP), 2.35 (s, 3H, CH_3 Mes), 2.16 (s, 6H, 2 CH_3 Mes), 1.27 (d, $^3J_{HP}$ = 13.4 Hz, 18H, 2 C(CH_3)$_3$), -17.90 (d, $^2J_{HP}$ = 66.5 Hz, 1H, NiH).

$^{13}C\{^1H\}$ NMR (101 MHz, THF-d_8): δ 185.0 (d, J_{CP} = 75 Hz, C-2 NHC), 169.5 (d, J_{CP} = 20 Hz, C_q arom), 152.5 (C_q arom), 139.7 (C_q arom), 138.8 (C_q arom), 136.3 (2 C_q arom), 134.3 (CH arom), 130.4 (2 CH arom), 124.0 (CH arom), 116.5 (CH arom), 114.2 (d, J_{CP} = 16 Hz, CH arom), 84.7 (CH arom), 65.6 (d, J_{CP} = 49 Hz, CHP), 35.7 (d, J_{CP} = 23 Hz, 2 C(CH_3)$_3$), 30.7 (d, J_{CP} = 5 Hz, 2 C(CH_3)$_3$), 22.0 (CH_3 Mes), 19.3 (2 CH_3 Mes).

$^{31}P\{^{1}H\}$ NMR (162 MHz, THF-d_8): δ 76.3 ppm.

IR (ATR): 1857 cm^{-1} (br, ν_{NiH}).

1.6. Synthesis and characterisation of nickel complexes 5

*Complex **5a***

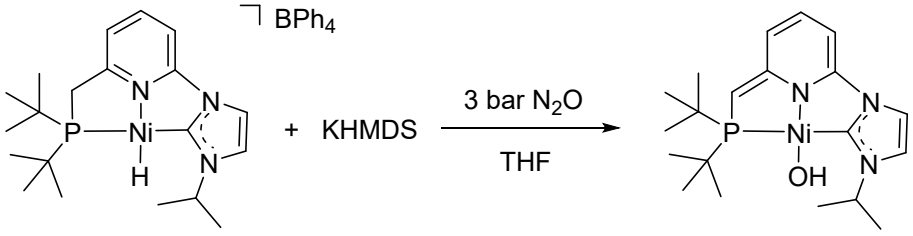

3a **5a**

In a Fisher−Porter vessel, a solution of complex **3a** (0.030 g, 0.04 mmol) in THF (5 mL) was treated with KHMDS (0.009 g, 0.05 mmol), and the mixture was stirred at room temperature for 12 h. After this time, the mixture was pressurized with 3 bar of N_2O, and stirred at 55 °C for 48 h. The system was depressurised, solvent was evaporated and the residue was extracted with Et_2O (2 x 7 mL). The desired product was obtained after evaporation of the solvent as a dark red solid (0.016 g, 90%). Satisfactory elemental analysis for this derivative could not be obtained due to partial decomposition during work-up.

^{1}H NMR (400 MHz, THF-d_8): δ 7.37 (s, 1H, H arom NHC), 7.21 (s, 1H, H arom NHC), 6.37 (dd, $^{3}J_{HH}$ = 8.7 Hz, $^{3}J_{HH}$ = 7.1 Hz, 1H, H arom Py), 5.88 (hept, 1H, $^{3}J_{HH}$ = 6.8 Hz, C*H*$(CH_3)_2$), 5.76 (d, $^{3}J_{HH}$ = 8.7 Hz, 1H, H arom Py), 5.32 (d, $^{3}J_{HH}$ = 7.1 Hz, 1H, H arom Py), 3.17 (s, 1H, CHP), 1.49 (d, $^{3}J_{HP}$ = 13.4 Hz, 18H, 2 C(C*H*$_3)_3$), 1.40 (d, $^{3}J_{HH}$ = 6.8 Hz, 6H, CH(C*H*$_3)_2$), -3.85 (d, $^{3}J_{HP}$ = 7.4 Hz, 1H, OH).

$^{13}C\{^{1}H\}$ NMR (101 MHz, THF-d_8): δ 170.9 (d, J_{CP} = 20 Hz, C_q arom), 168.8 (d, J_{CP} = 101 Hz, C-2 NHC), 152.1 (C_q arom), 133.6 (CH arom), 119.1 (d, J_{CP} = 4 Hz, CH arom), 115.1 (CH arom), 112.9 (d, J_{CP} = 16 Hz, CH arom), 86.1 (CH arom), 63.1 (d, J_{CP} = 54 Hz, CHP), 49.1 (*C*H$(CH_3)_2$), 36.7 (d, J_{CP} = 19 Hz, 2 *C*$(CH_3)_3$), 30.3 (d, J_{CP} = 4 Hz, 2 C(*C*H$_3)_3$), 24.3 (2 CH(*C*H$_3)_2$).

$^{31}P\{^{1}H\}$ NMR (162 MHz, THF-d_8): δ 43.2 ppm.

IR (ATR): 3649 cm^{-1} (br, ν_{OH}).

*Complex **5b***

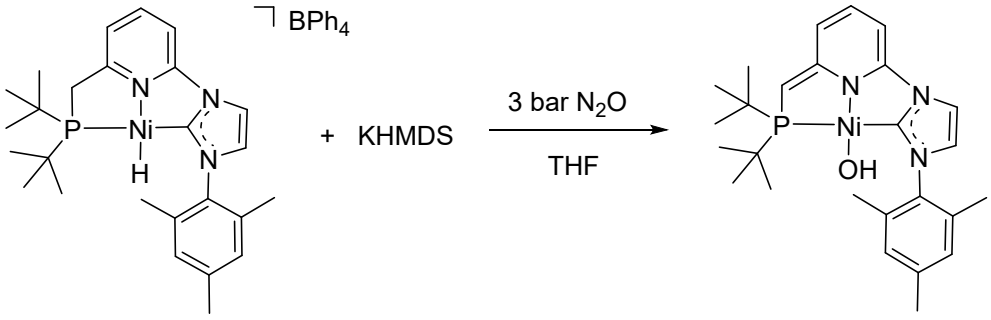

3b **5b**

In a Fisher−Porter vessel, a solution of complex **3b** (0.030 g, 0.04 mmol) in THF (5 mL) was treated with KHMDS (0.008 g, 0.04 mmol), and the mixture was stirred at room temperature for 12 h. After this time, the solution was pressurized with 3 bar of N_2O and stirred at 55 °C for 48 h. The system was depressurised, solvent was evaporated and the residue was extracted with Et_2O (2 x 7 mL). The desired product was obtained after evaporation of the solvent as a dark red solid (0.017 g, 90%). Satisfactory elemental analysis for this derivative could not be obtained due to partial decomposition during work-up. Crystals suitable for X-ray diffraction analysis were obtained by slow evaporation of Et_2O solutions of the complex.

^{1}H NMR (400 MHz, THF-d_8): δ 7.65 (s, 1H, H arom NHC), 7.04 (s, 1H, H arom NHC), 7.02 (s, 2 H, H arom Mes), 6.38 (dd, $^3J_{HH}$ = 9.0 Hz, $^3J_{HH}$ = 7.0 Hz, 1H, H arom Py), 5.80 (d, $^3J_{HH}$ = 9.0 Hz, 1H, H arom Py), 5.41 (d, $^3J_{HH}$ = 7.0 Hz, 1H, H arom Py), 3.22 (s, 1H, CHP), 2.33 (s, 3H, CH_3 Mes), 2.28 (s, 6H, 2 CH_3 Mes), 1.43 (d, $^3J_{HP}$ = 12.7 Hz, 18H, 2 C(CH_3)$_3$), -3.73 (d, $^3J_{HP}$ = 3.2 Hz, 1H, OH).

^{13}C{^{1}H} NMR (101 MHz, THF-d_8): δ 171.7 (d, J_{CP} = 102 Hz, C-2 NHC), 170.9 (d, J_{CP} = 20 Hz, C_q arom), 151.4 (d, J_{CP} = 6 Hz, C_q arom), 140.9 (C_q arom), 136.8 (2 C_q arom), 135.7 (C_q arom), 133.1 (CH arom), 130.9 (2 CH arom), 124.6 (d, J_{CP} = 4 Hz, CH arom), 116.0 (CH arom), 113.6 (d, J_{CP} = 16 Hz, CH arom), 86.1 (CH arom), 64.3 (d, J_{CP} = 50 Hz, CHP), 36.7 (d, J_{CP} = 18 Hz, 2 C(CH_3)$_3$), 30.0 (d, J_{CP} = 4 Hz, 2 C(CH_3)$_3$), 22.0 (CH_3 Mes), 18.8 (2 CH_3 Mes).

^{31}P{^{1}H} NMR (162 MHz, THF-d_8): δ 44.3 ppm.

IR (ATR): 3599 cm^{-1} (br, ν_{OH}).

1.7. Representative procedure of N_2O reduction with pinacolborane

In a glovebox, a J.Young valved NMR tube was charged with 37 μL of a freshly prepared 0.025 M stock solution of **3b** (0.9 μmol) in THF-d_8, 11 μL of a 0.1 M stock solution of KHMDS (1.1 μmol) in THF-d_8, and 0.4 mL of THF-d_8 . Then, pinacolborane (27 μL, 0.19 mmol) and mesitylene (5 μL) were added, and the nitrogen atmosphere in the tube was replaced by 2 bar of N_2O by performing three freeze-pump-thaw cycles. The reaction progress, pinBOH:$(pinB)_2O$ ratio, and H_2 formation (not quantified) were determined by ^1H and/or $^{11}B\{^1H\}$ NMR spectroscopies. H_2 evolution is expected to arise from the formation of $(pinB)_2O$ by reaction of pinacolborane and pinBOH.[2,3] In a control experiment using catalytic amounts of KHMDS in the absence of the Ni precursors, conversion of HBpin to the corresponding oxidation products was not observed.

Hg test: In a glovebox, a J.Young valved NMR tube was charged with 37 μL of a freshly prepared 0.025 M stock solution of **3b** (0.9 μmol) in THF-d_8, 11 μL of a 0.1 M stock solution of KHMDS (1.1 μmol) in THF-d_8, and 0.4 mL of THF-d_8 . Then, pinacolborane (27 μL, 0.19 mmol), Hg (0.010 g, 0.05 mmol; 53 equiv) and mesitylene (5 μL) were added, and the nitrogen atmosphere in the tube was replaced by 2 bar of N_2O by performing three freeze-pump-thaw cycles. The reaction progress was monitored by ^1H and $^{11}B\{^1H\}$ NMR spectroscopies, and found to proceed as the experiment in entry 4, Table 1 (2.5 h: >99% conv; pinBOH:$(pinB)_2O$ ratio = 2:8).

To qualitatively determine the formation of N_2, a GC−MS analysis of the gas atmosphere was carried out using a Shimadzu GCMS-TQ8040 apparatus equipped with a PoraBOND Q capillary column (25 m, 0.25 mm i.d., 3 *μ*m film thickness). Helium carrier gas was supplied at a head pressure of 3.7 psi to provide an initial flow rate of 4.6 mL/min. The injector temperature was set up to 200 °C, and the oven temperature was initially held at 30 °C for 5 min, then gradually increased to 150 °C at 25 °C/min. Full-scan mass spectra were collected from *m*/*z* 10 to 50 at a data acquisition rate of 158 spectra/s. The MS transfer line was held at 250 °C, and the ion source temperature was 200 °C.

---

[2] Y. Pang, M. Leutzsch, N. Nöthling and J. Cornella, *J. Am. Chem. Soc.*, 2020, **142**, 19473.

[3] X. Chen, H. Wang, S. Du, M. Driess and Z. Mo, *Angew. Chem. Int. Ed.*, 2022, **61***,* e202114598

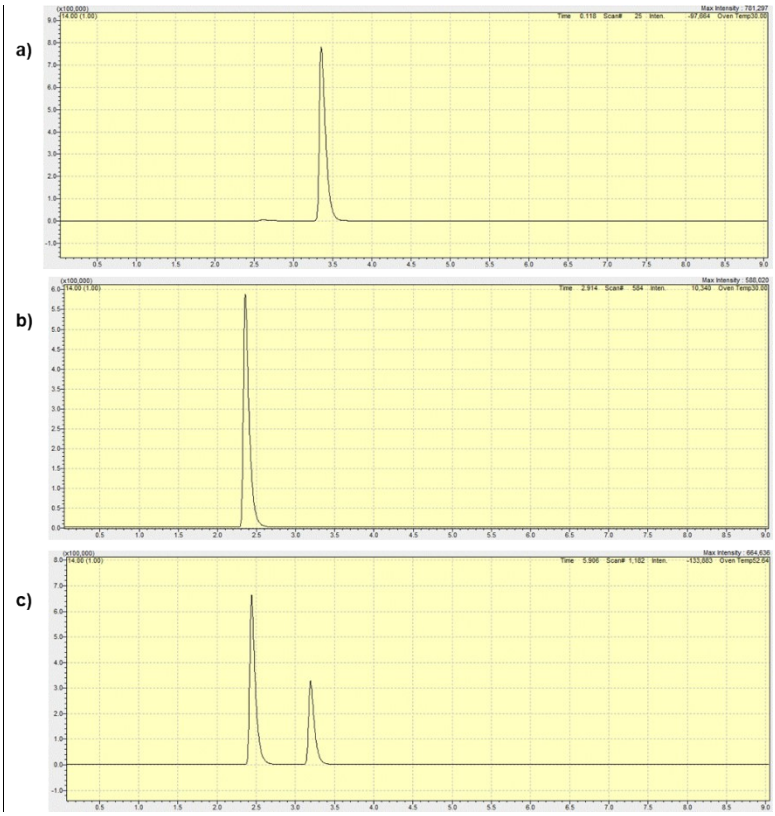

Figure S1. N_2 determination by GC-MS: a) control experiment N_2O; b) control experiment N_2; c) catalytic reaction (Table 1, entry 4).

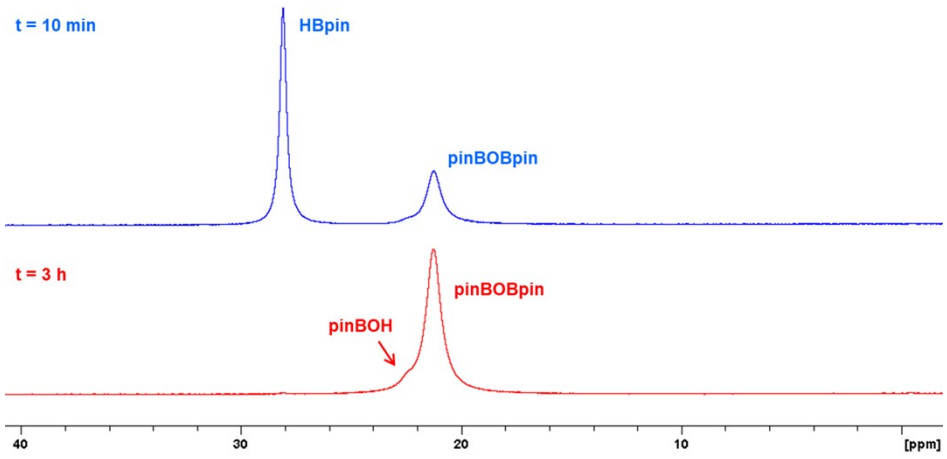

Figure S2. $^{11}B\{^1H\}$ NMR spectrum (128 MHz) of the reaction of N_2O (2 bar) with pinacolborane in THF-d_8 catalysed by **4a** (Table 1, entry 3).

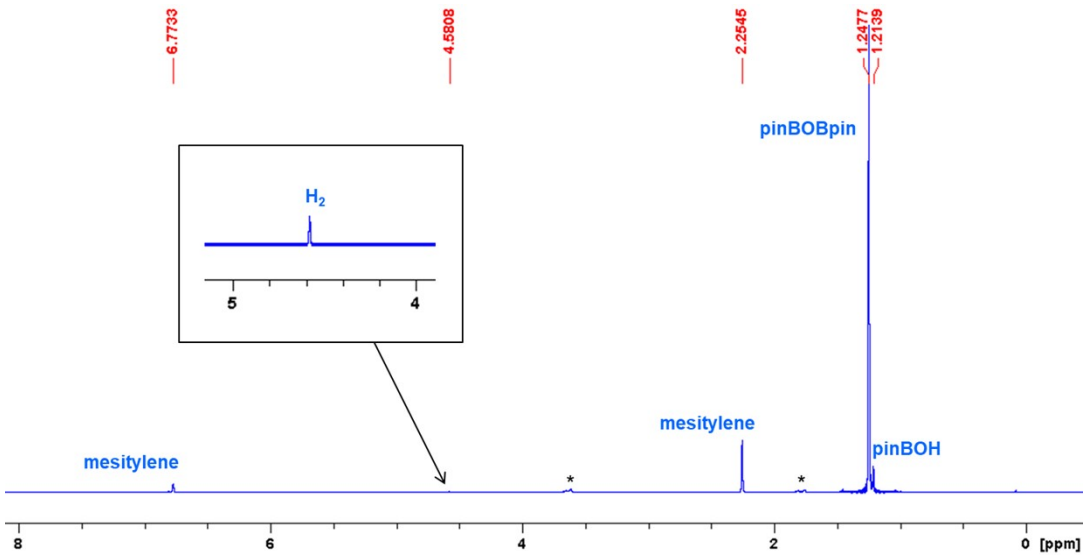

Figure S3. ^{1}H NMR spectrum (300 MHz) of the reaction of N_2O (2 bar) with pinacolborane in THF-d_8 catalysed by **4a** (Table 1, entry 3). (* solvent residual signals).

2. X-Ray structure analysis of complexes 3a and 5b

Crystals suitable for X-ray diffraction analysis were coated with dry perfluoropolyether, mounted on glass fibres, and fixed in a cold nitrogen stream to the goniometer head. Data collections[4] were performed on a Bruker-AXS, D8 Quest ECO diffractometer equipped with a micro-focus IμS 3.0 source, using graphite monochromatized Mo radiation λ(Mo Kα) = 0.71073 Å and with an area detector Bruker Photon II 14 - CPAD. The data were reduced (*SAINT*) and corrected for absorption effects by the multiscan method (*SADABS*).[5] The structures were solved by direct methods (*SIR2002*, *SHELXS*)[6] and refined against all F^2 data by full-matrix least-squares techniques (*SHELXL*-2018/3)[7] minimizing $w[F_o^2\text{-}F_c^2]^2$. All non-hydrogen atoms were refined with anisotropic displacement parameters. Hydrogen atoms were included in calculated positions and allowed to ride on their carrier atoms with the isotropic temperature factors U_{iso} fixed at 1.2 times (1.5 times for methyl groups) of the U_{eq} values of the respective carrier atoms.

The crystal structure of **3a** crystallises in the centrosymmetric space group $P2_1/c$. In the crystal's asymmetric unit, only one salt of the Ni(II) complex is present, comprising the BPh_4 anion and the cationic CPN Ni(II) hydride complex. Both tert-butyl groups of the phosphine ligands exhibit disorder in the carbon atoms of the methyl groups. While these disorders did not necessitate explicit modelling, they did require the application of anisotropic displacement parameter (ADP) restraints. The crystal structure of **5b** crystallises in the centrosymmetric space group $P4_2/n$. In the asymmetric unit of this crystal, a single Ni(II) hydroxide complex is observed, revealing that the methylene bridge of the CNP pincer ligand is mono-deprotonated. A search for solvent accessible voids for this crystal structure **5b** using SQUEEZE[8] showed 2 small volumes of potential solvents of 179 Å^3 for each, whose solvent content could not be identified or refined with the most severe restraints. The corresponding CIF data represent SQUEEZE treated structures with the solvent molecules handling as a diffuse contribution to the overall scattering, without specific atom position and excluded from the structural model. The SQUEEZE results were appended to the CIF. A summary of cell parameters, data collection, structure solution, and refinement for these two crystal structures are given in

[4] Bruker APEX3 software suite; Bruker AXS, Inc.; Madison, WI 53711, 2016.

[5] Bruker Advanced X-ray solutions. *SAINT* and *SADABS* programs. Bruker AXS Inc. Madison, WI 53711, **2012**.

[6] M. C. Burla, M. Camalli, B. Carrozzini, G. L. Cascarano, C. Giacovazzo, G. Polidori and R. Spagna, *J. Appl. Crystallogr.*, 2003, **36**, 1103−1104.

[7] G. M. Sheldrick, *Acta Crystallogr. Sect. A*, 2008, **64**,112−122.

[8] P. v.d. Sluis, A. L. Spek, *Acta Crystallogr., Sect. A*, 1990, **46**, 194−201.

Tables S1 and S2. The corresponding crystallographic data were deposited with the Cambridge Crystallographic Data Centre as supplementary publications. CCDC 2299058 (**3a**) and CCDC 2299059 (**5b**) contain the supplementary crystallographic data for this paper. These data can be obtained free of charge from The Cambridge Crystallographic Data Centre via www.ccdc.cam.ac.uk/data_request/cif.

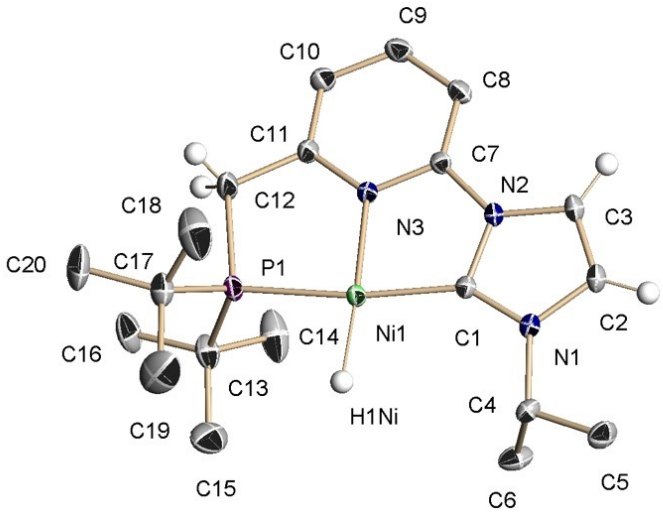

Figure S4. ORTEP view of molecular structure of complex **3a** with thermal ellipsoids depicted at the 30% probability level. Hydrogen atoms, with the exception of the Ni-hydride, NHC, and pincer linker hydrogens, have been omitted for clarity. Selected bond lengths [Å] and angles [°]: Ni(1)–C(1) 1.8852(13), Ni(1)–N(3) 1.9093(11), Ni(1)–P(1) 2.1533(4), Ni(1)–H(1HNi) 1.6212, C(1)–Ni(1)–N(3) 83.21(5), N(3)–Ni(1)–P(1) 87.35(4), C(1)–Ni(1)–H(1HNi) 99.6, P(1)–Ni(1)–H(1HNi) 89.9.

Table S1. Crystal data and structure refinement for **3a**.

Empirical formula	$C_{44}H_{54}BN_3NiP$	
	$[C_{20}H_{33}N_3NiP, C_{24}H_{20}B]$	
Formula weight	725.39	
Temperature	193(2) K	
Wavelength	0.71073 Å	
Crystal system	Monoclinic	
Space group	$P2_1/c$	
Unit cell dimensions	a = 14.5193(4) Å	α = 90°.
	b = 29.0183(7) Å	β = 103.8940(10)°.
	c = 9.5279(2) Å	γ = 90°.
Volume	3896.89(17) $Å^3$	
Z	4	
Density (calculated)	1.236 Mg/m^3	
Absorption coefficient	0.573 mm^{-1}	
F(000)	1548	
Crystal size	0.400 x 0.350 x 0.100 mm^3	
Theta range for data collection	2.014 to 30.527°.	
Index ranges	-20<=h<=20, -41<=k<=41, -13<=l<=13	
Reflections collected	167470	
Independent reflections	11915 [R(int) = 0.0352]	
Completeness to theta = 25.242°	99.9 %	
Absorption correction	Semi-empirical from equivalents	
Max. and min. transmission	0.7461 and 0.4770	
Refinement method	Full-matrix least-squares on F^2	
Data / restraints / parameters	11915 / 36 / 459	
Goodness-of-fit on F^2	1.039	
Final R indices [I>2sigma(I)]	R1 = 0.0392, wR2 = 0.1093	
R indices (all data)	R1 = 0.0448, wR2 = 0.1139	
Extinction coefficient	n/a	
Largest diff. peak and hole	0.990 and -0.476 e.$Å^{-3}$	

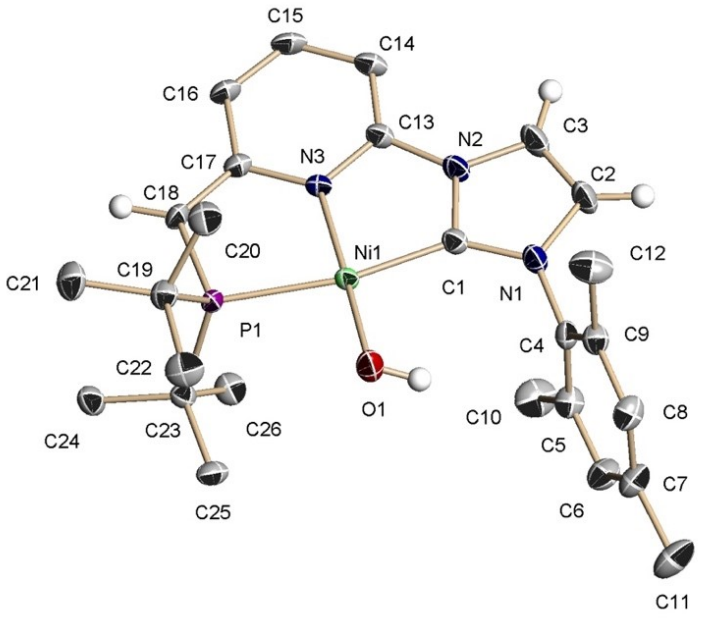

Figure S5. ORTEP view of molecular structure of complex **5b** with thermal ellipsoids depicted at the 30% probability level. Hydrogen atoms, except Ni-hydroxyl, NHC, and one pincer linker hydrogen, have been omitted for clarity. Selected bond lengths [Å] and angles [°]: Ni(1)–C(1) 1.905(2), Ni(1)–N(3) 1.8839(19), Ni(1)–P(1) 2.2246(7), Ni(1)–O(1) 1.8272(18), C(1)–Ni(1)–N(3) 82.05(9), N(3)–Ni(1)–P(1) 84.84(6), C(1)–Ni(1)–O(1) 99.89(9), P(1)–Ni(1)–O(1) 93.35(6).

Table S2. Crystal data and structure refinement for **5b**.

Empirical formula	$C_{26}H_{36}N_3NiOP$	
Formula weight	496.26	
Temperature	193(2) K	
Wavelength	0.71073 Å	
Crystal system	Tetragonal	
Space group	$P4_2/n$	
Unit cell dimensions	a = 21.355(2) Å	α = 90°.
	b = 21.355(2) Å	β = 90°.
	c = 11.6688(15) Å	γ = 90°.
Volume	5321.2(14) $Å^3$	
Z	8	
Density (calculated)	1.239 Mg/m^3	
Absorption coefficient	0.811 mm^{-1}	
F(000)	2112	
Crystal size	0.200 x 0.100 x 0.080 mm^3	
Theta range for data collection	1.907 to 25.237°.	
Index ranges	-25<=h<=25, -25<=k<=25, -14<=l<=14	
Reflections collected	175281	
Independent reflections	4813 [R(int) = 0.0908]	
Completeness to theta = 25.237°	100.0 %	
Absorption correction	Semi-empirical from equivalents	
Max. and min. transmission	0.7461 and 0.6756	
Refinement method	Full-matrix least-squares on F^2	
Data / restraints / parameters	4813 / 0 / 299	
Goodness-of-fit on F^2	1.039	
Final R indices [I>2sigma(I)]	R1 = 0.0373, wR2 = 0.0932	
R indices (all data)	R1 = 0.0463, wR2 = 0.0974	
Extinction coefficient	n/a	
Largest diff. peak and hole	0.898 and -0.456 e.$Å^{-3}$	

3. Selected NMR spectra of nickel complexes

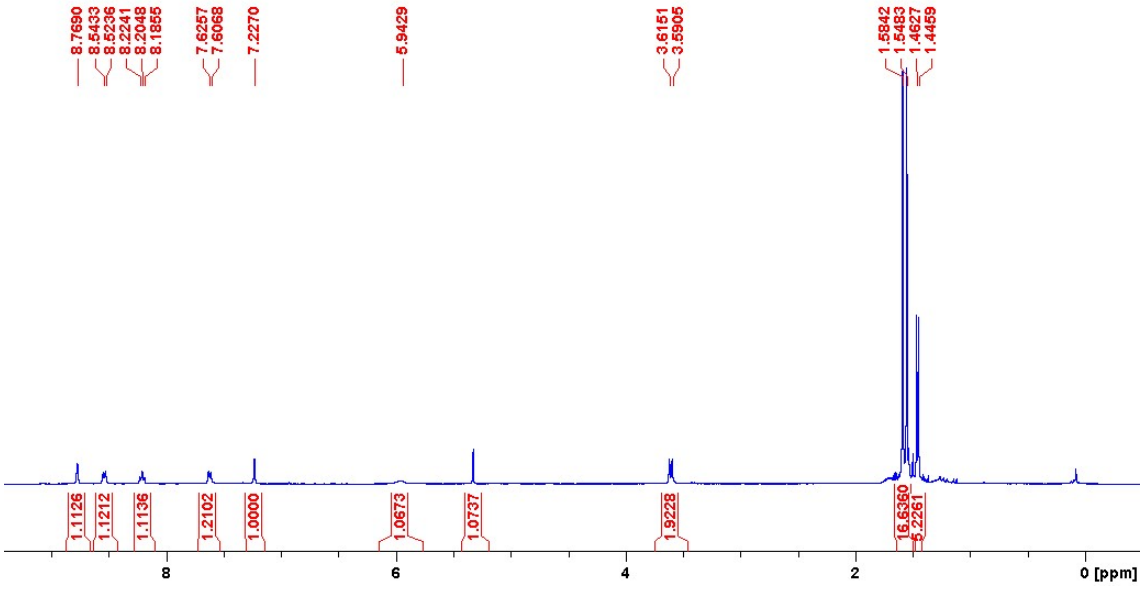

Figure S6. ^{1}H NMR spectrum (400 MHz) of **2a** in CD_2Cl_2.

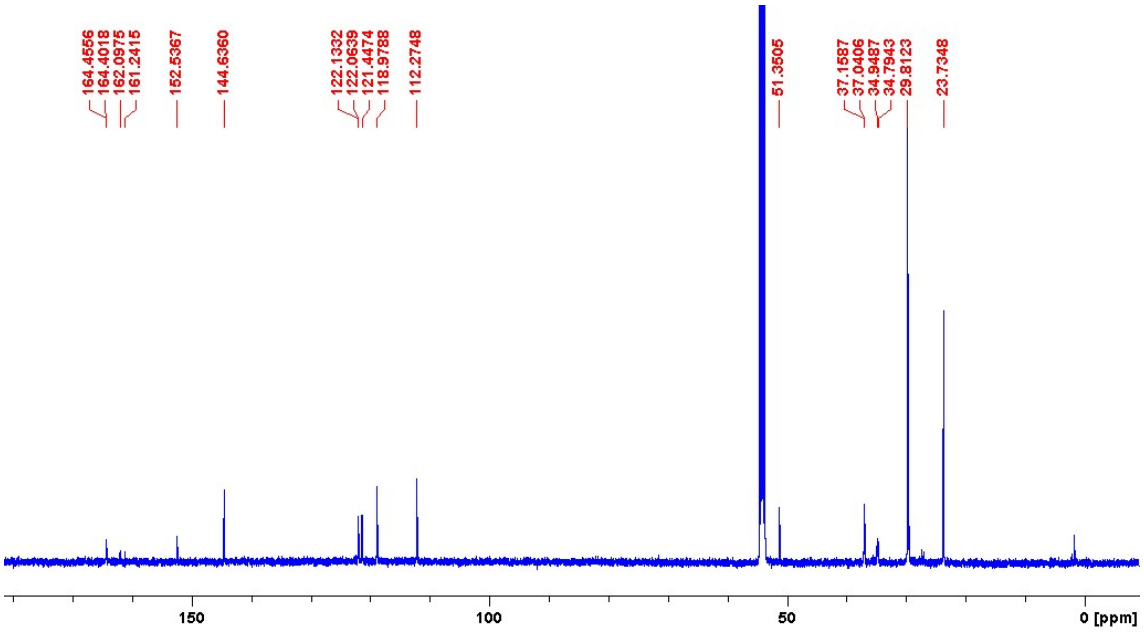

Figure S7. $^{13}C\{^{1}H\}$ NMR spectrum (101 MHz) of **2a** in CD_2Cl_2.

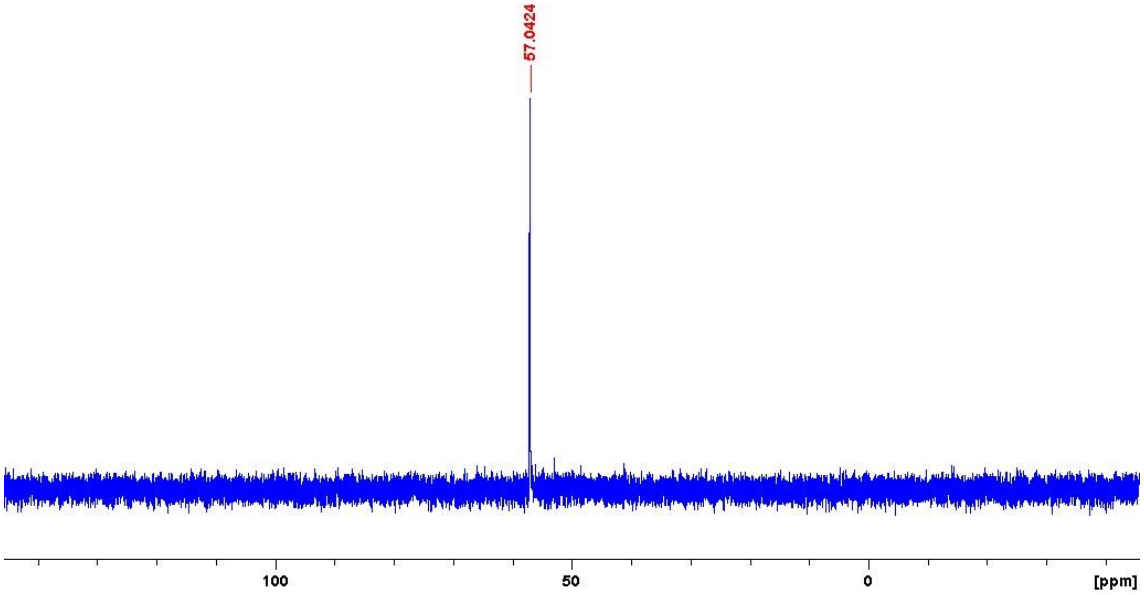

Figure S8. $^{31}P\{^{1}H\}$ NMR spectrum (162 MHz) of **2a** in THF-d_8.

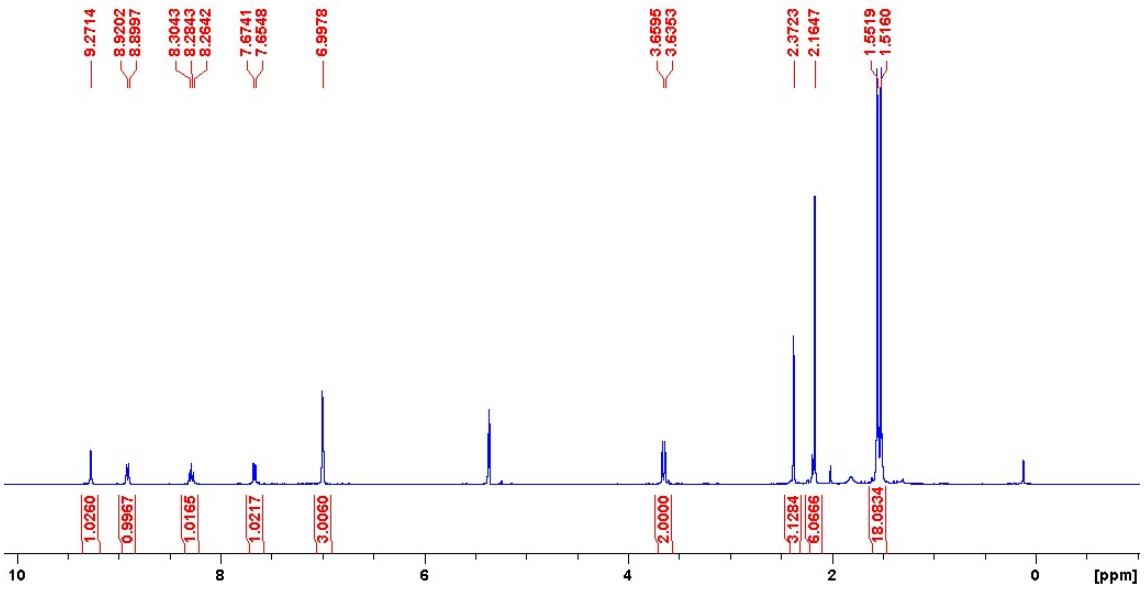

Figure S9. ^{1}H NMR spectrum (400 MHz) of **2b** in CD_2Cl_2.

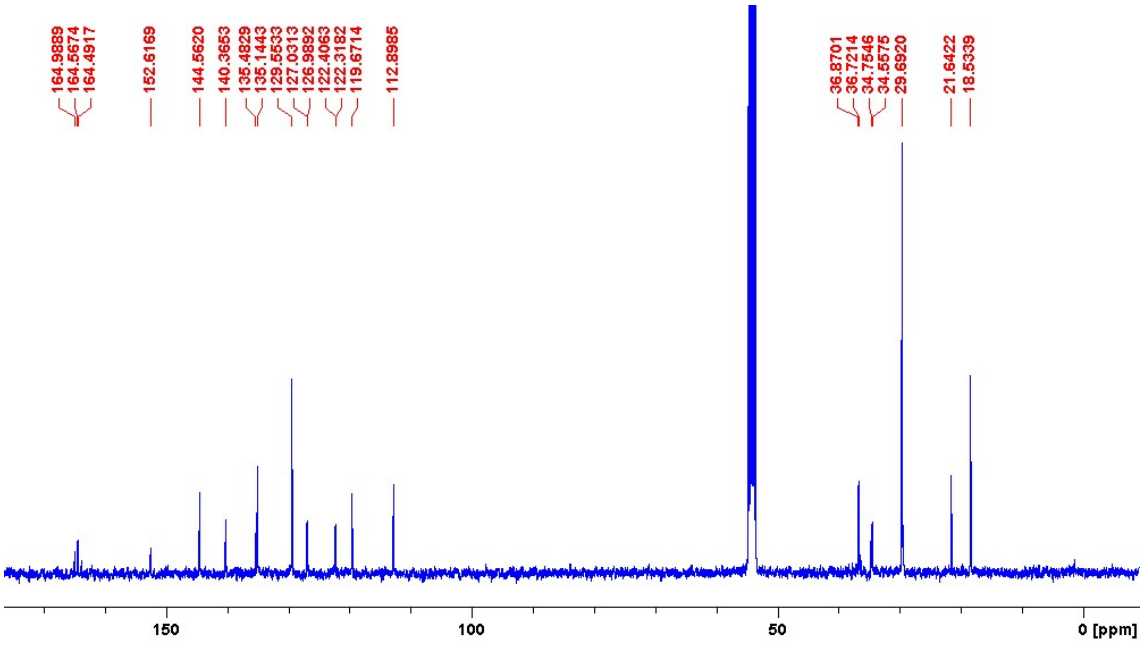

Figure S10. $^{13}C\{^{1}H\}$ NMR spectrum (101 MHz) of **2b** in CD_2Cl_2.

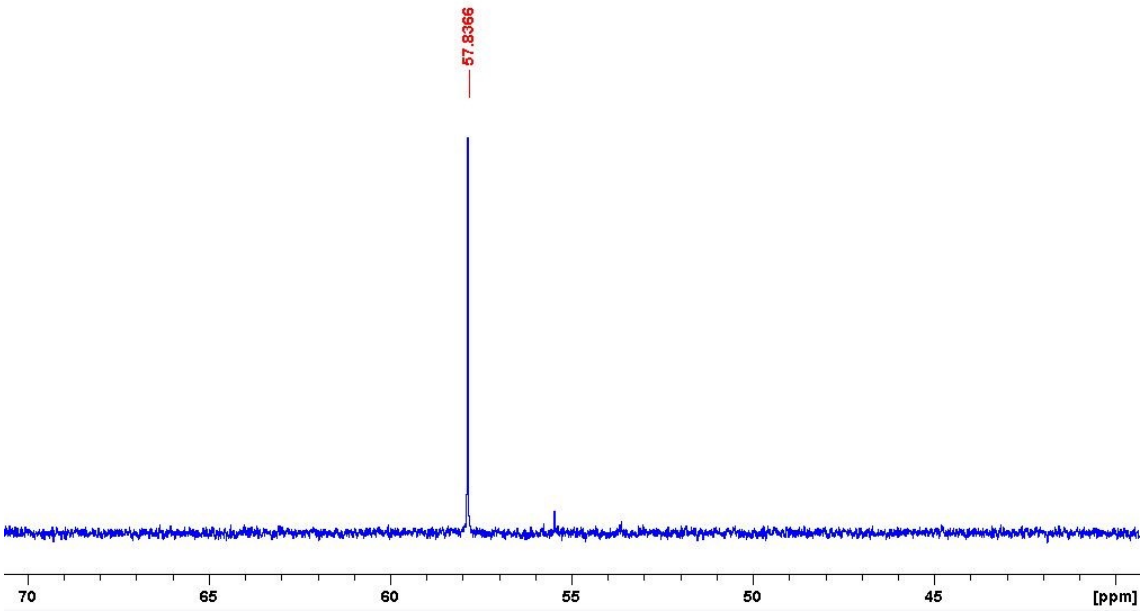

Figure S11. $^{31}P\{^{1}H\}$ NMR spectrum (162 MHz) of **2b** in CD_3CN.

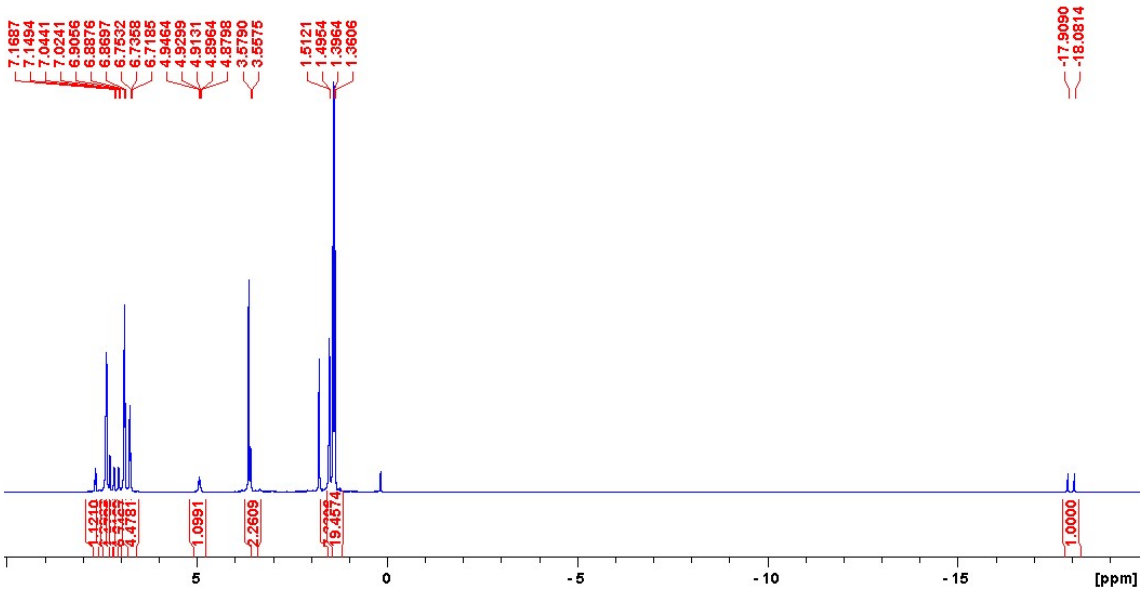

Figure S12. ^{1}H NMR spectrum (400 MHz) of **3a** in THF-d_8.

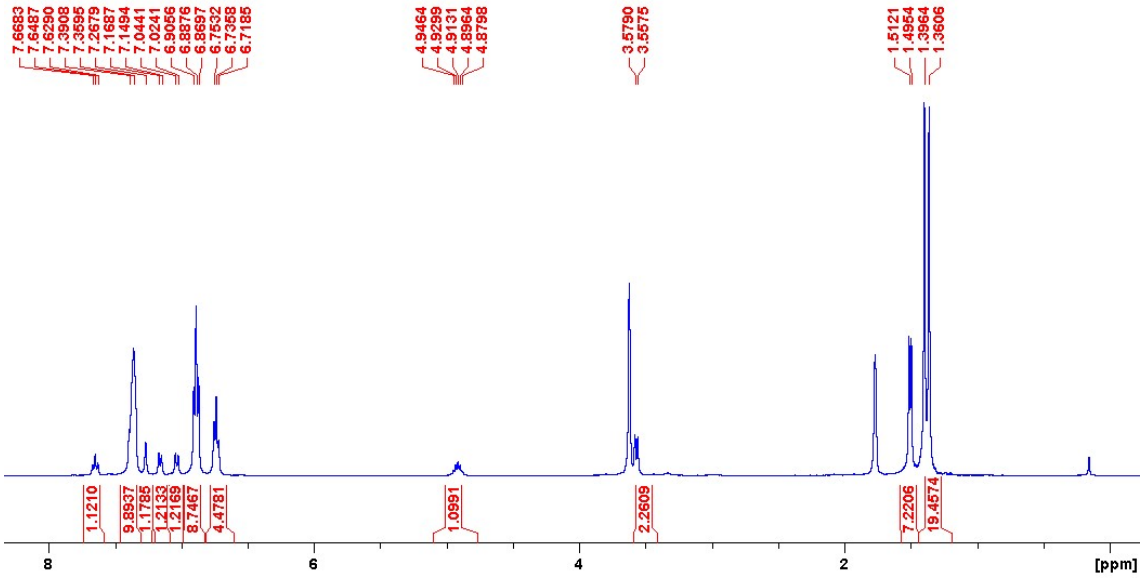

Figure S13. Region (0.0 - 8.0 ppm) of the ^{1}H NMR spectrum (400 MHz) of **3a** in THF-d_8.

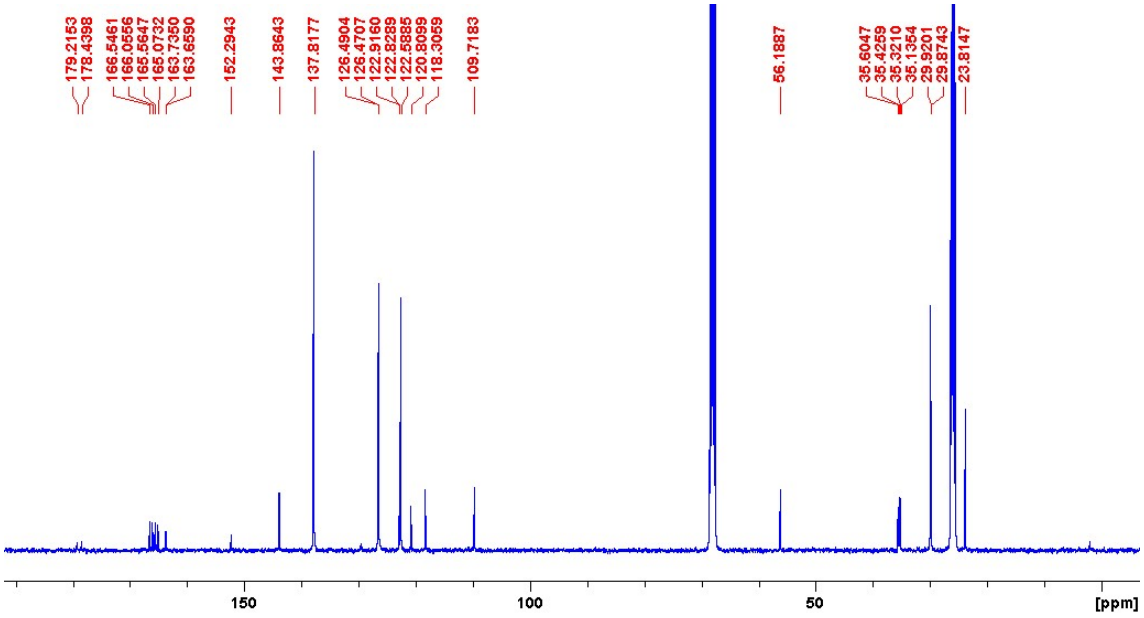

Figure S14. $^{13}C\{^{1}H\}$ NMR spectrum (101 MHz) of **3a** in THF-d_8.

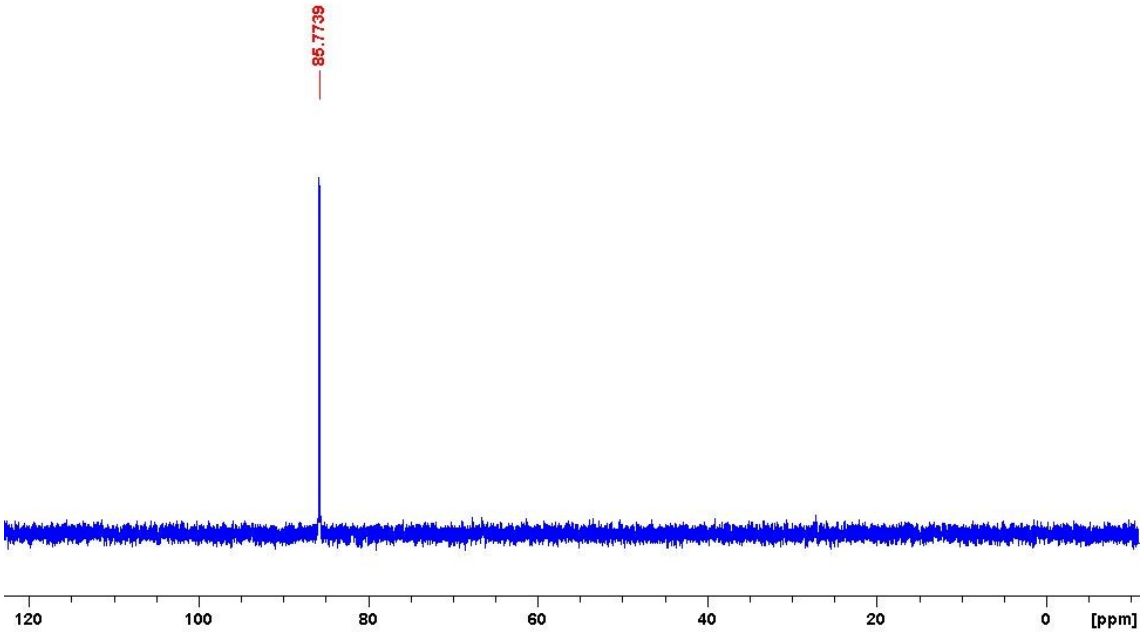

Figure S15. $^{31}P\{^{1}H\}$ NMR spectrum (162 MHz) of **3a** in THF-d_8.

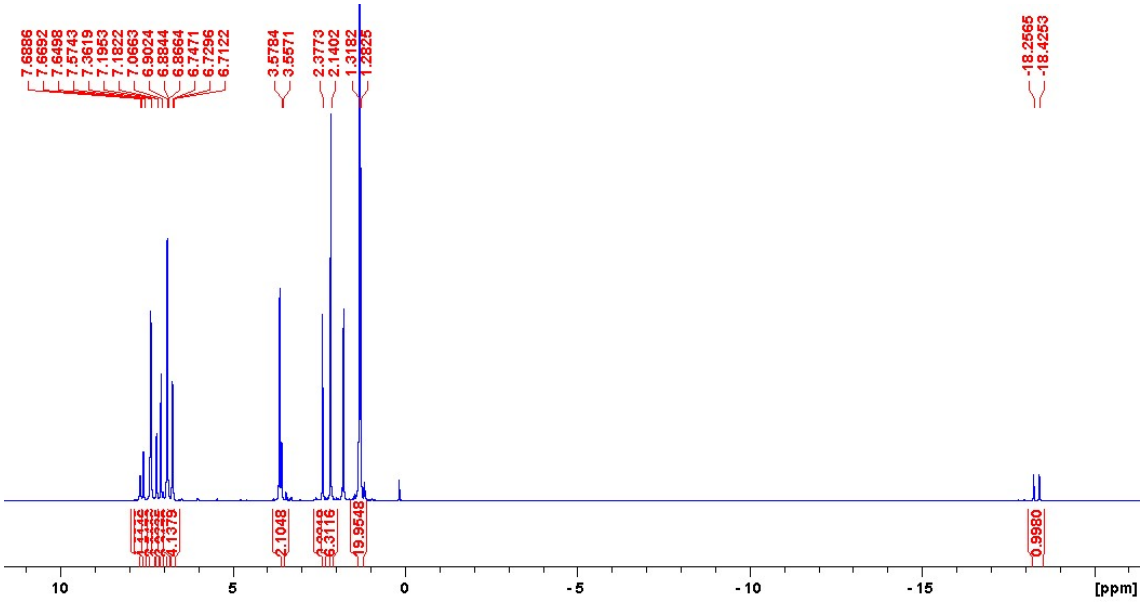

Figure S16. ^{1}H NMR spectrum (400 MHz) of **3b** in THF-d_8.

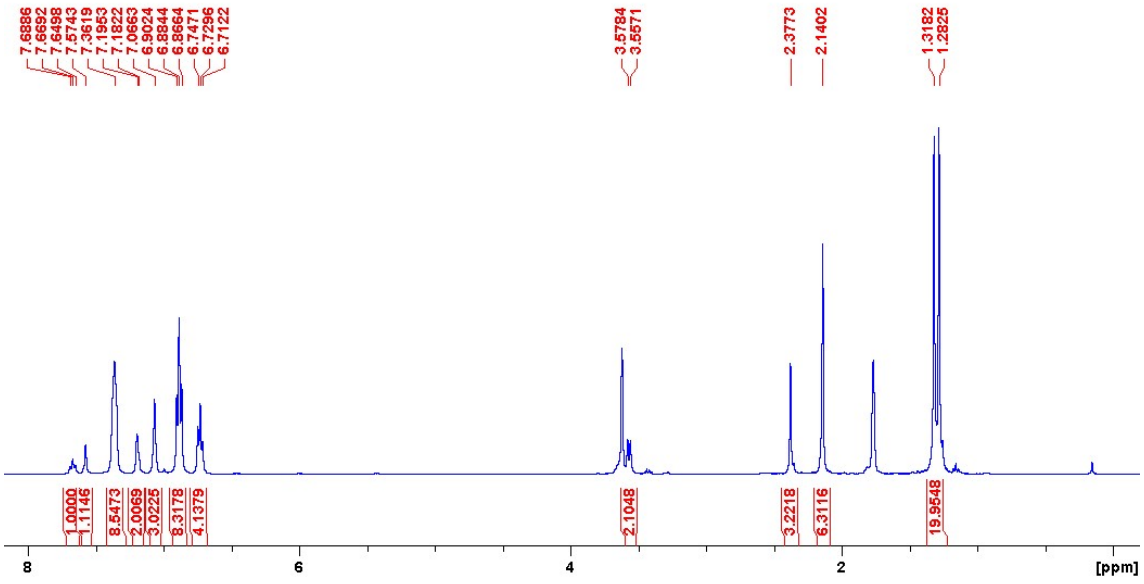

Figure S17. Region (0.0-8.0 ppm) of the ^{1}H NMR spectrum (400 MHz) of **3b** in THF-d_8.

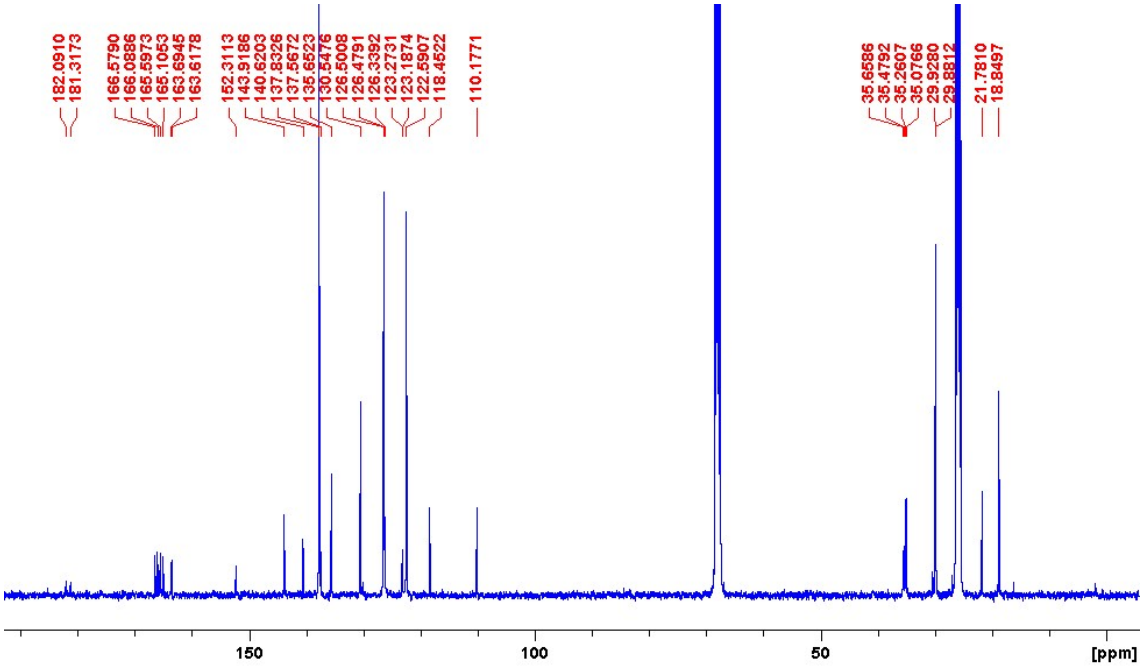

Figure S18. $^{13}C\{^{1}H\}$ NMR spectrum (101 MHz) of **3b** in THF-d_8.

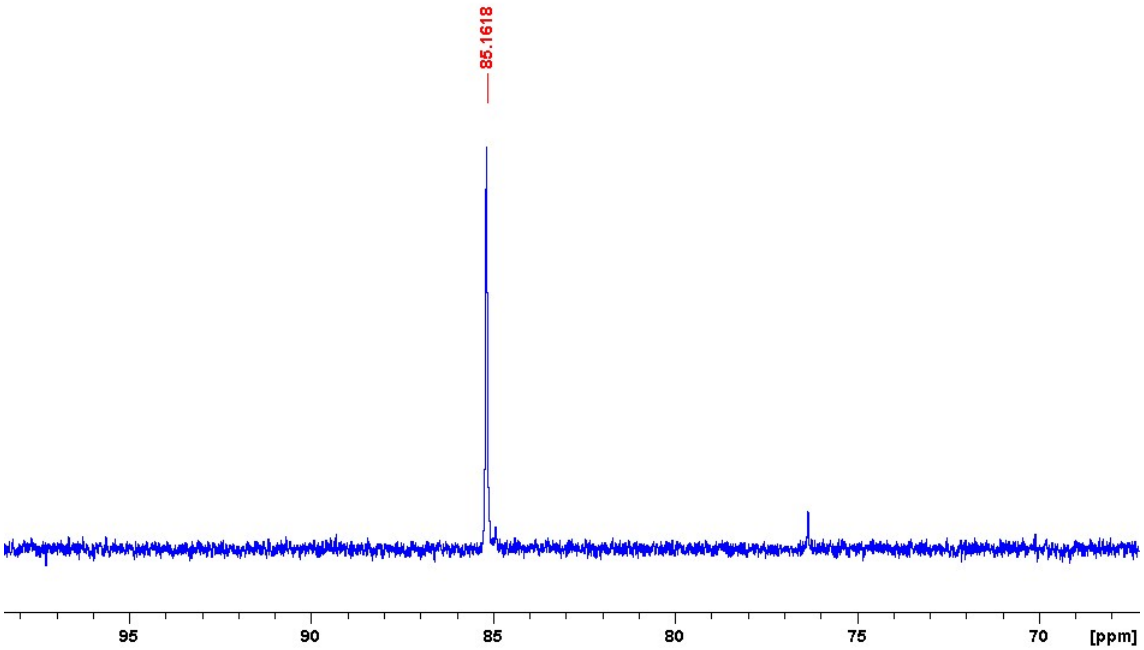

Figure S19. $^{31}P\{^{1}H\}$ NMR spectrum (162 MHz) of **3b** in CD_3CN.

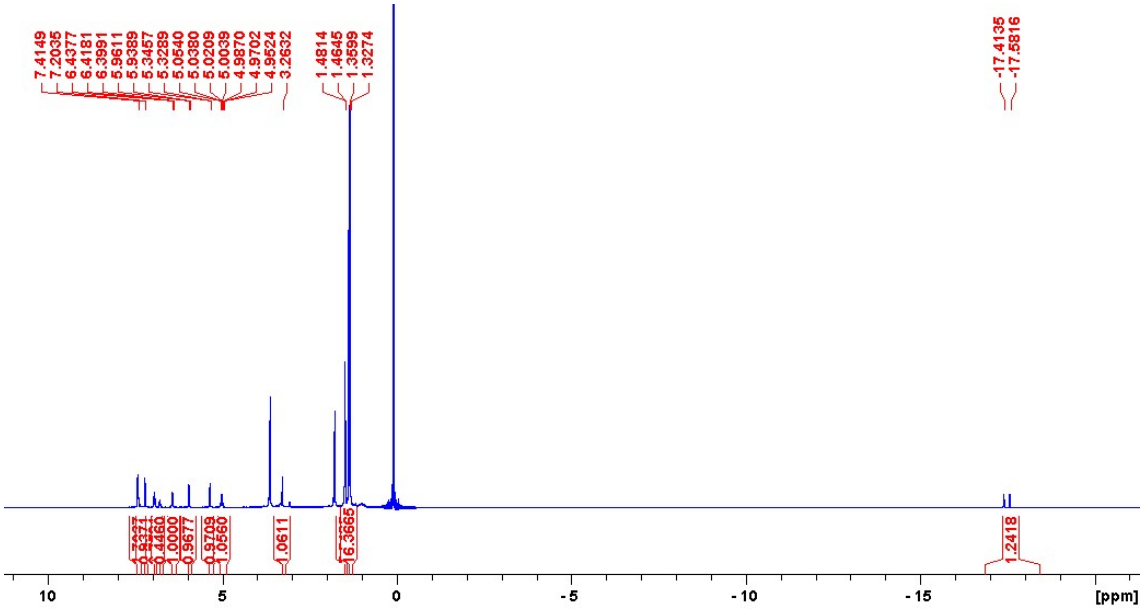

Figure S20. ^{1}H NMR spectrum (400 MHz) of **4a** in THF-d_8 (contains signals corresponding to the BPh_4^- anion and HMDS).

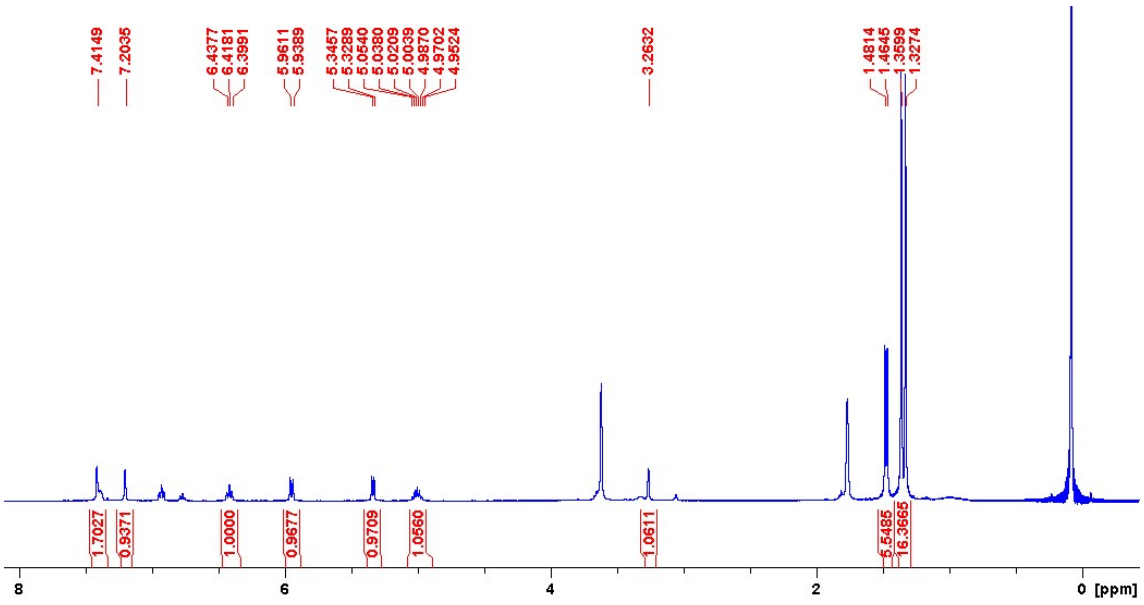

Figure S21. Region (0.0-8.0 ppm) of the ^{1}H NMR spectrum (400 MHz) of **4a** in THF-d_8 (contains signals corresponding to the BPh_4^- anion and HMDS).

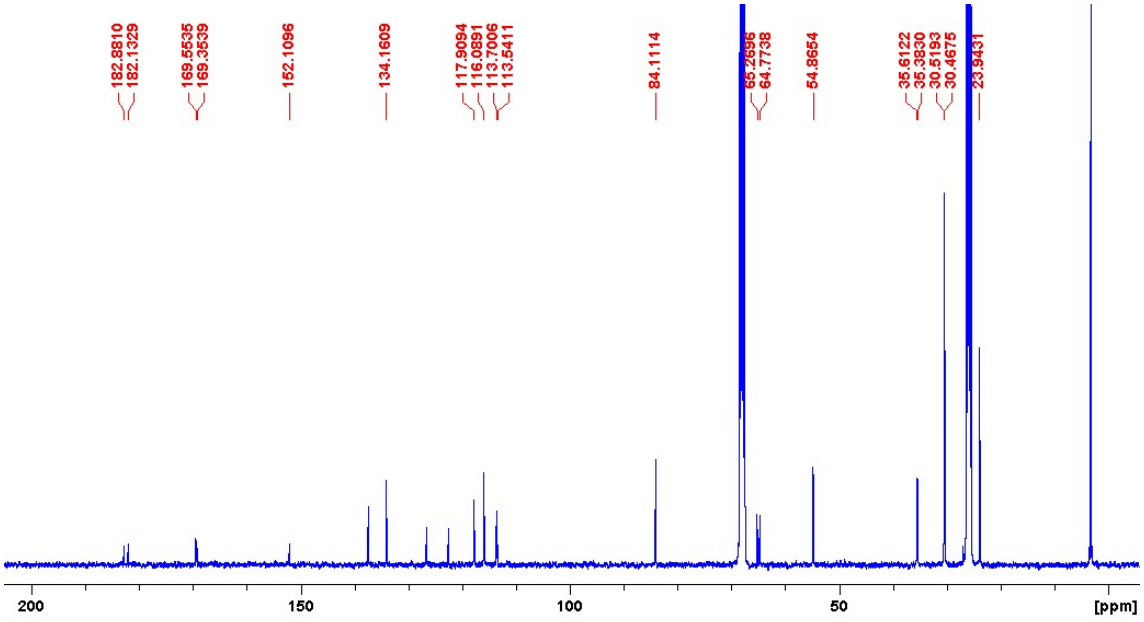

Figure S22. $^{13}C\{^{1}H\}$ NMR spectrum (101 MHz) of **4a** in THF-d_8 (contains signals corresponding to the BPh_4^- anion and HMDS).

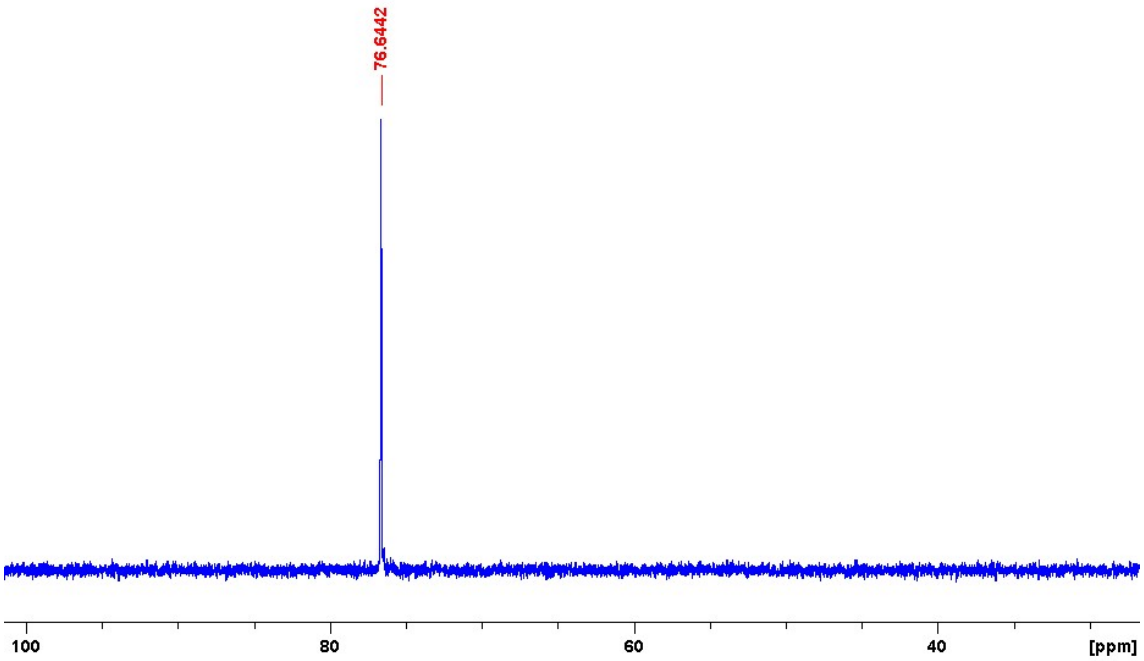

Figure S23. $^{31}P\{^{1}H\}$ NMR spectrum (162 MHz) of **4a** in THF-d_8.

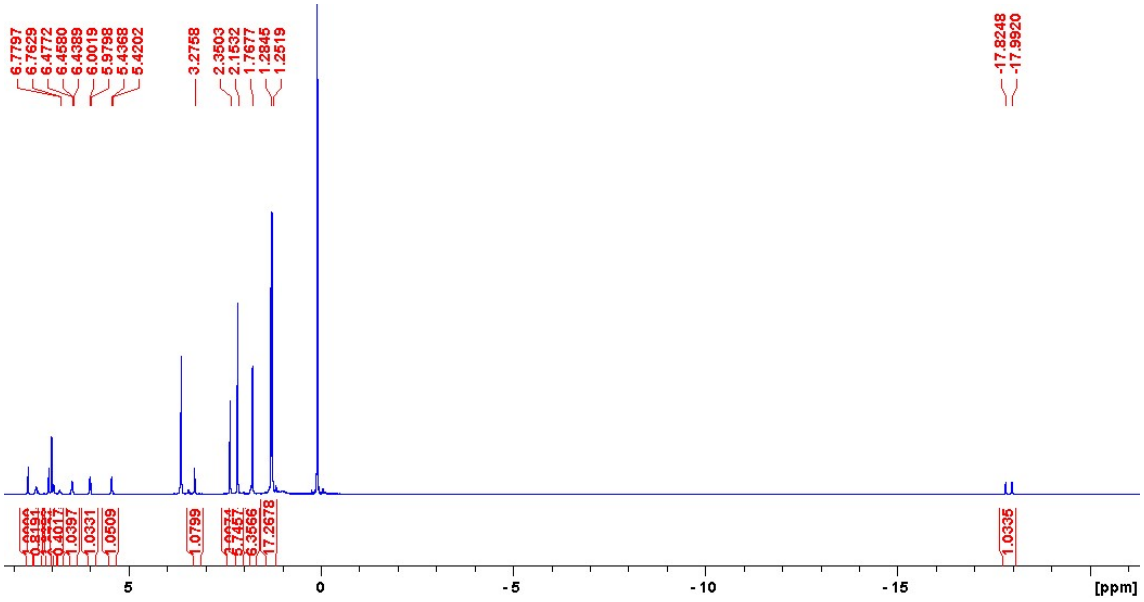

Figure S24. ^{1}H NMR spectrum (400 MHz) of **4b** in THF-d_8 (contains signals corresponding to the BPh_4^- anion and HMDS).

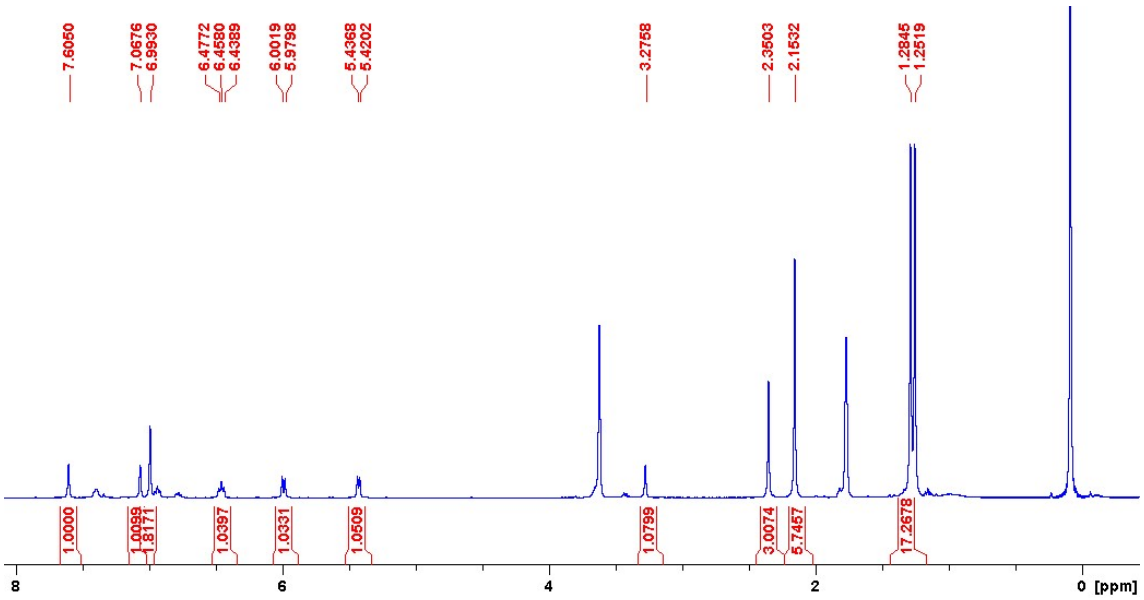

Figure S25. Region (0.0 to 8.0 ppm) of the ^{1}H NMR spectrum (400 MHz) of **4b** in THF-d_8 (contains signals corresponding to the BPh_4^- anion and HMDS).

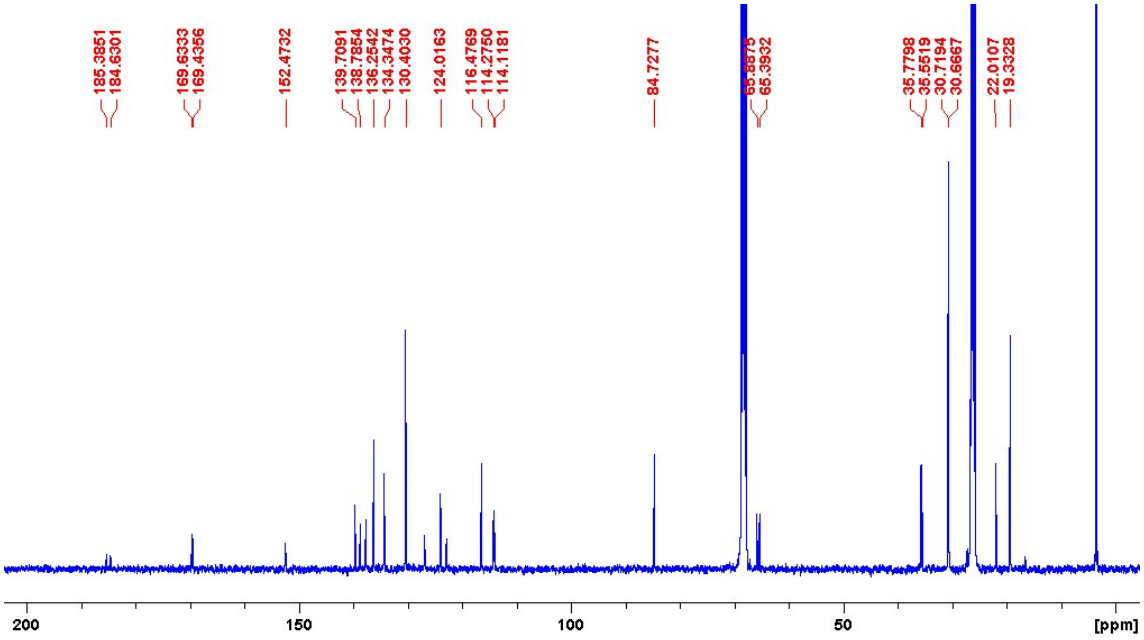

Figure S26. $^{13}C\{^{1}H\}$ NMR spectrum (101 MHz) of **4b** in THF-d_8 (contains signals corresponding to the BPh_4^- anion and HMDS).

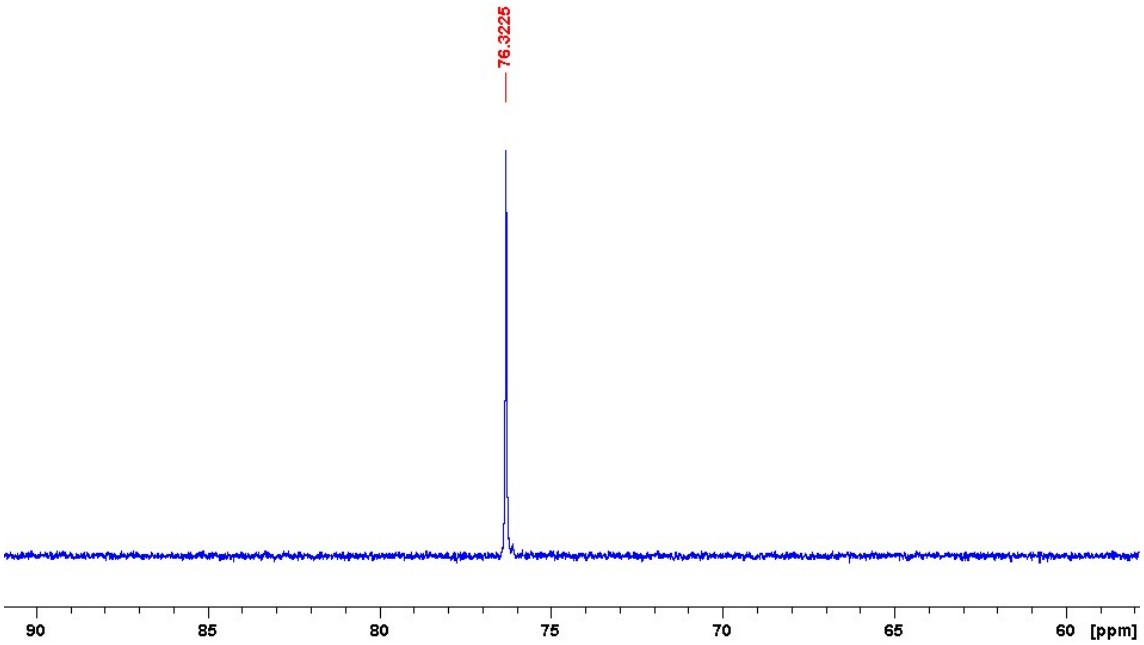

Figure S27. $^{31}P\{^{1}H\}$ NMR spectrum (162 MHz) of **4b** in THF-d_8.

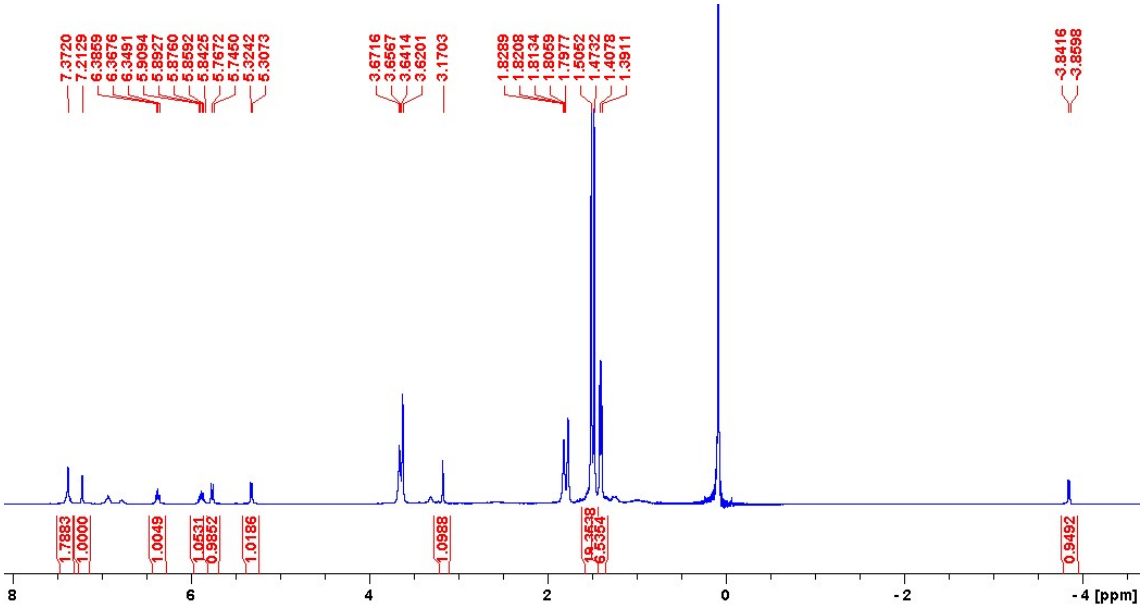

Figure S28. ^{1}H NMR spectrum (400 MHz) of **5a** in THF-d_8 (contains signals corresponding to the BPh_4^- anion and HMDS).

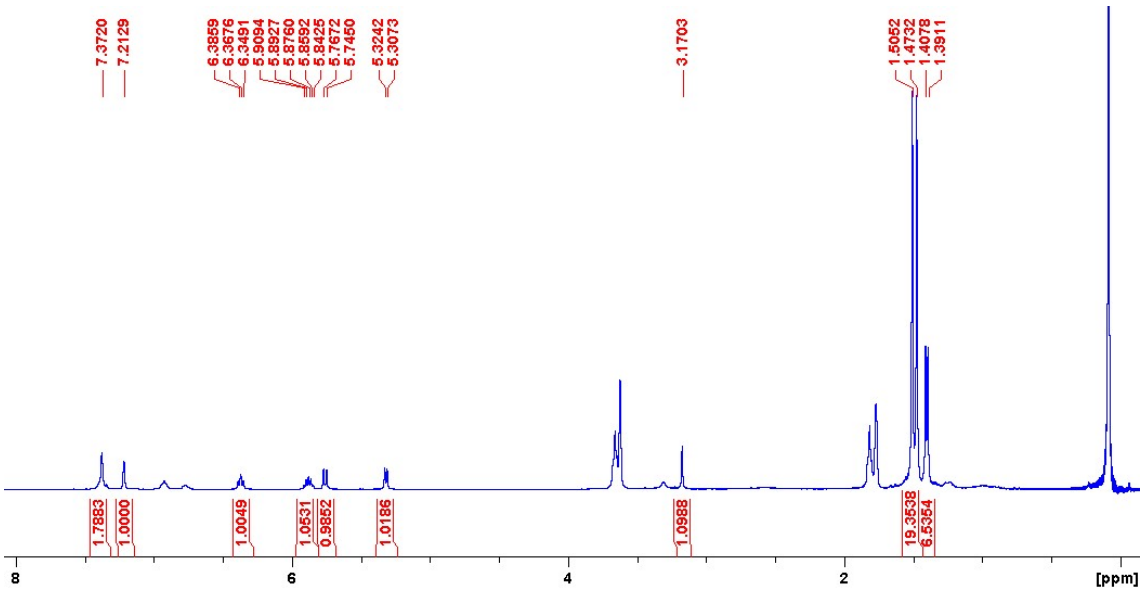

Figure S29. Region (0.0-8.0 ppm) of the ^{1}H NMR spectrum (400 MHz) of **5a** in THF-d_8 (contains signals corresponding to the BPh_4^- anion and HMDS).

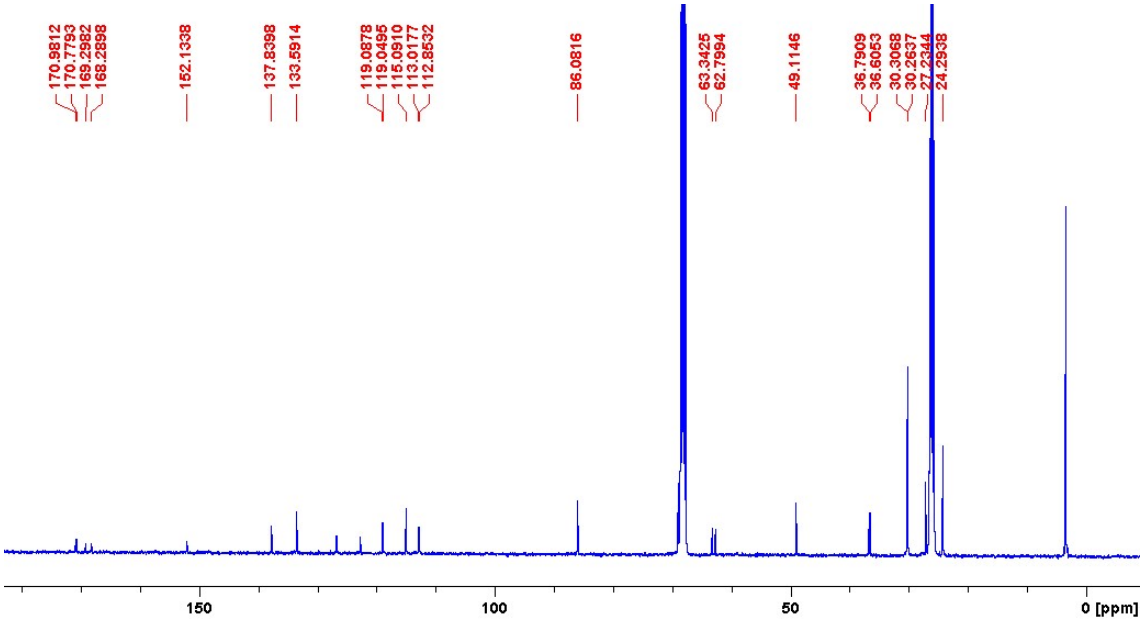

Figure S30. $^{13}C\{^{1}H\}$ NMR spectrum (101 MHz) of **5a** in THF-d_8 (contains signals corresponding to the BPh_4^- anion and HMDS).

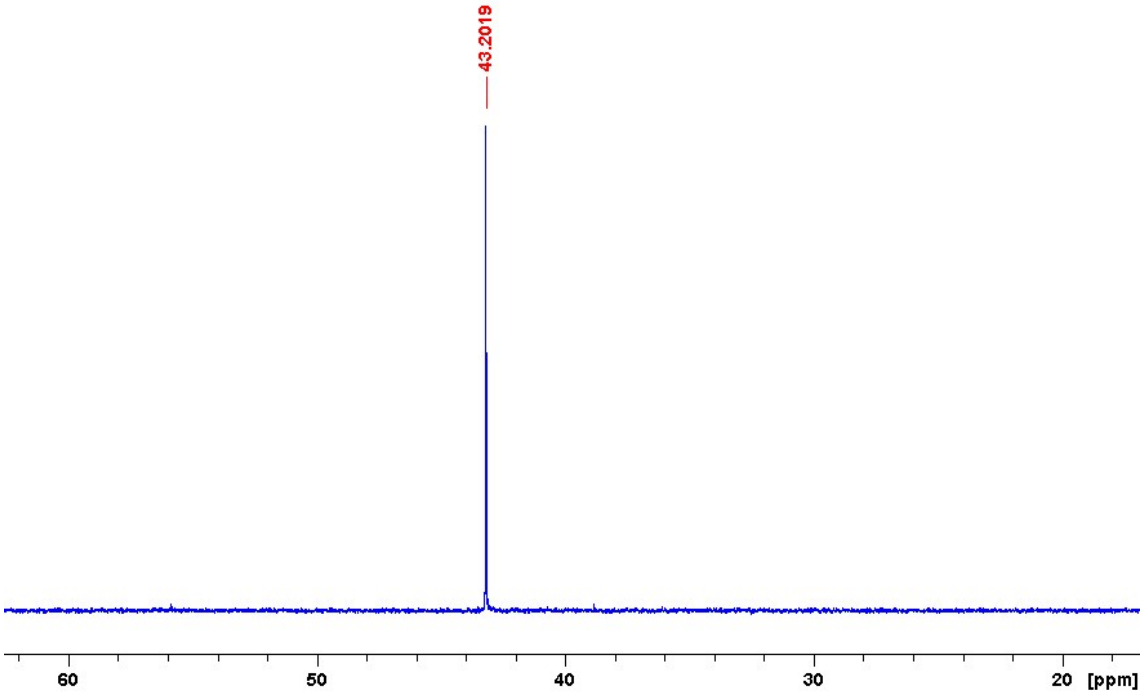

Figure S31. $^{31}P\{^{1}H\}$ NMR spectrum (162 MHz) of **5a** in THF-d_8.

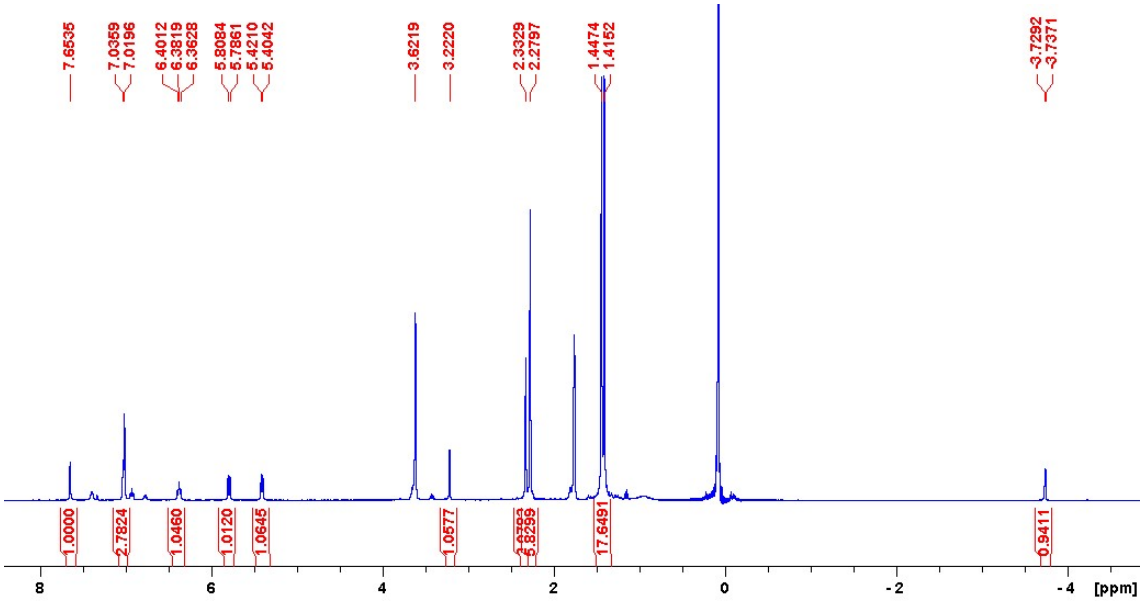

Figure S32. ^{1}H NMR spectrum (400 MHz) of **5b** in THF-d_8 (contains signals corresponding to the BPh_4^- anion and HMDS).

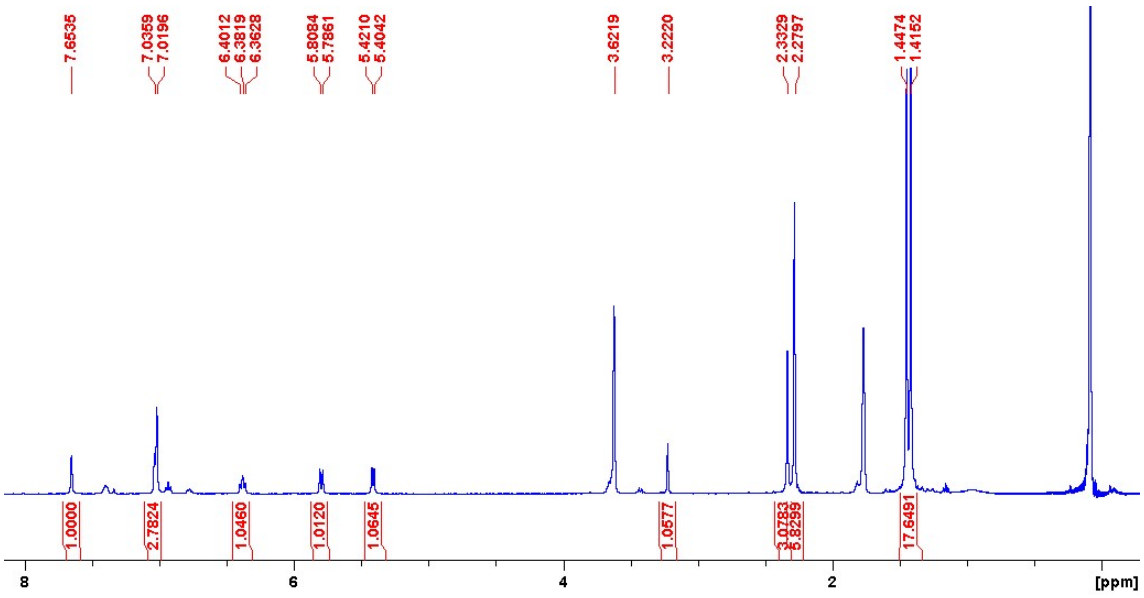

Figure S33. Region (0.0-8.0 ppm) of the ^{1}H NMR spectrum (400 MHz) of **5b** in THF-d_8 (contains signals corresponding to the BPh_4^- anion and HMDS).

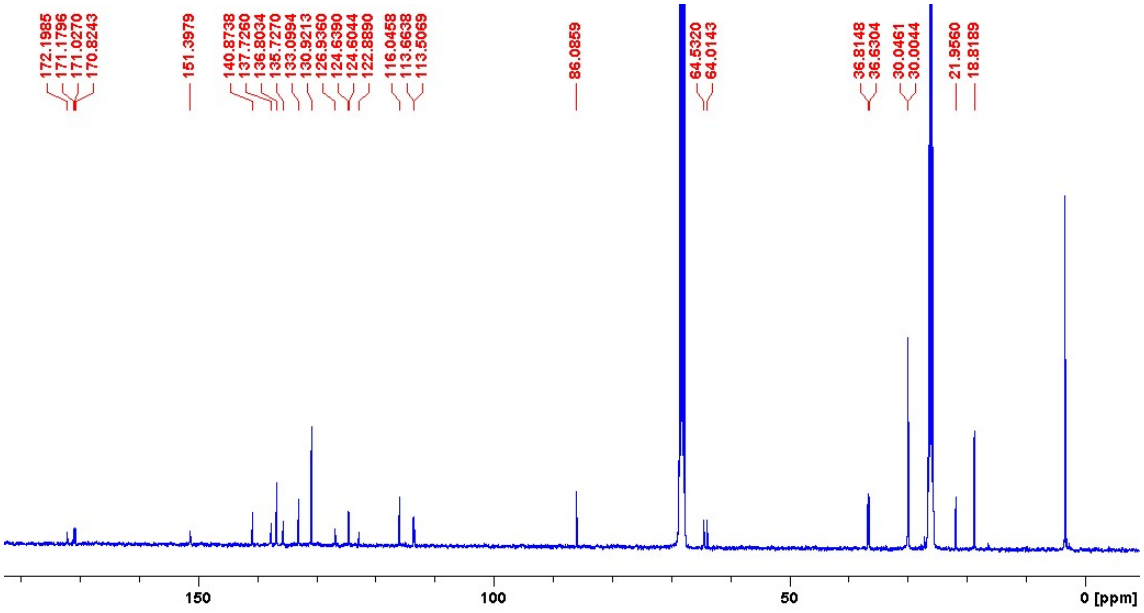

Figure S34. $^{13}C\{^{1}H\}$ NMR spectrum (101 MHz) of **5b** in THF-d_8 (contains signals corresponding to the BPh_4^- anion and HMDS).

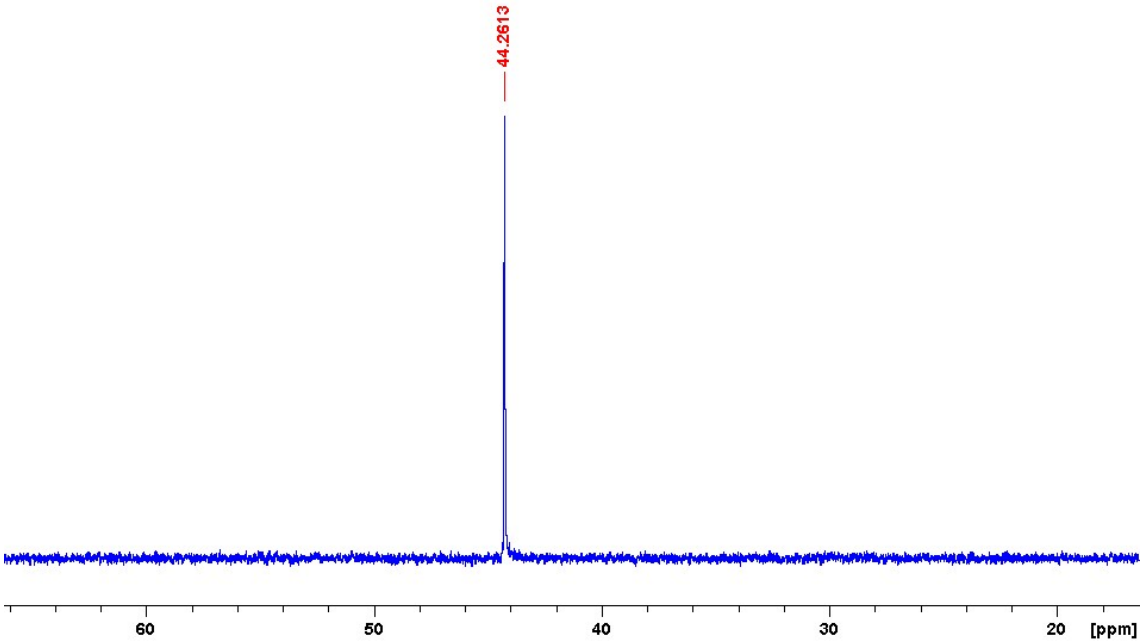

Figure S35. $^{31}P\{^{1}H\}$ NMR spectrum (162 MHz) of **5b** in THF-d_8.

4. DFT calculations

Calculations were carried out at the DFT level using the Gaussian 09 program[9] with the B3LYP hybrid functional,[10] with dispersion effects taken into account by adding the D3 version of Grimme's empirical dispersion.[11] All atoms were represented with the Def2TZVP basis set.[12] All geometry optimizations were performed in bulk solvent (THF) without restrictions. Vibrational analysis was used to characterise the stationary points in the potential energy surface, as well as for calculating the zero-point, enthalpy, and Gibbs energy corrections at 295 K and 1 atm. The nature of the intermediates connected by a given transition state along a reaction path was proven by intrinsic reaction coordinate (IRC) calculations or by perturbing the geometry of the TS along the reaction path eigenvector. Bulk solvent effects were modelled with the SMD continuum model.[13]

---

[9] Frisch, M. J.; Trucks, G. W.; Schlegel, H. B.; Scuseria, G. E.; Robb, M. A.; Cheeseman, J. R.; Scalmani, G.; Barone, V.; Petersson, G. A.; Nakatsuji, H.; Li, X.; Caricato, M.; Marenich, A.; Bloino, J.; Janesko, B. G.; Gomperts, R.; Mennucci, B.; Hratchian, H. P.; Ortiz, J. V.; Izmaylov, A. F.; Sonnenberg, J. L.; Williams-Young, D.; Ding, F.; Lipparini, F.; Egidi, F.; Goings, J.; Peng, B.; Petrone, A.; Henderson, T.; Ranasinghe, D.; Zakrzewski, V. G.; Gao, J.; Rega, N.; Zheng, G.; Liang, W.; Hada, M.; Ehara, M.; Toyota, K.; Fukuda, R.; Hasegawa, J.; Ishida, M.; Nakajima, T.; Honda, Y.; Kitao, O.; Nakai, H.; Vreven, T.; Throssell, K.; Montgomery, J. A., Jr.; Peralta, J. E.; Ogliaro, F.; Bearpark, M.; Heyd, J. J.; Brothers, E.; Kudin, K. N.; Staroverov, V. N.; Keith, T.; Kobayashi, R.; Normand, J.; Raghavachari, K.; Rendell, A.; Burant, J. C.; Iyengar, S. S.; Tomasi, J.; Cossi, M.; Millam, J. M.; Klene, M.; Adamo, C.; Cammi, R.; Ochterski, J. W.; Martin, R. L.; Morokuma, K.; Farkas, O.; Foresman, J. B.; Fox, D. J. *Gaussian 09*, revision E.01; Gaussian, Inc.: Wallingford, CT, 2016.

[10] (a) A. D. Becke, *J. Chem. Phys.*, 1993, **98**, 5648−5652; (b) C. Lee, W. Yang and R. G. Parr, *Phys. Rev. B: Condens. Matter Mater. Phys.*, 1988, **37**, 785−789; (c) B. Miehlich, A. Savin, H. Stoll and H. Preuss, *Chem. Phys. Lett.*, 1989, **157**, 200−206.

[11] S. Grimme, S. Ehrlich and L. Goerigk, *J. Comput. Chem.,* 2011, **32**, 1456−1465.

[12] (a) F. Weigend and R. Ahlrichs, *Phys. Chem. Chem. Phys.*, 2005, **7**, 3297−3305; (b) F. Weigend, *Phys. Chem. Chem. Phys.*, 2006, **8**, 1057−1065.

[13] A. V. Marenich, C. J. Cramer and D. G. Truhlar, *J. Phys. Chem. B*, 2009, **113**, 6378−6396.

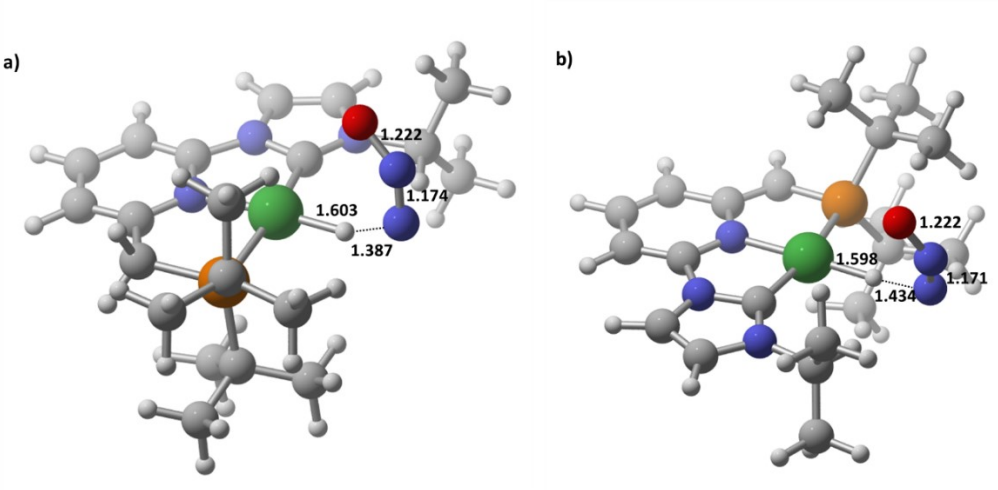

Figure S36. Views of the DFT-optimized geometries of the transition states **TS(3a→A)** (a) and **TS(4a→A*)** (b).

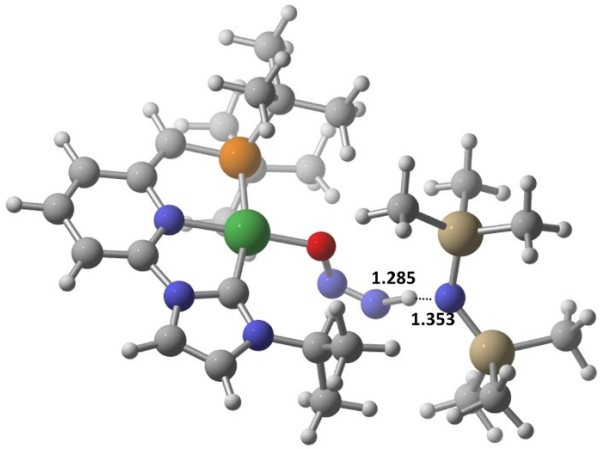

Figure S37. View of the DFT-optimized geometry of the transition state **TS(A*→C*)**.

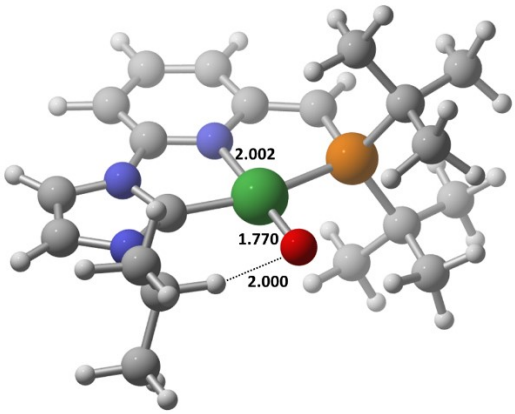

Figure S38. View of the DFT-optimized geometry of **C***.

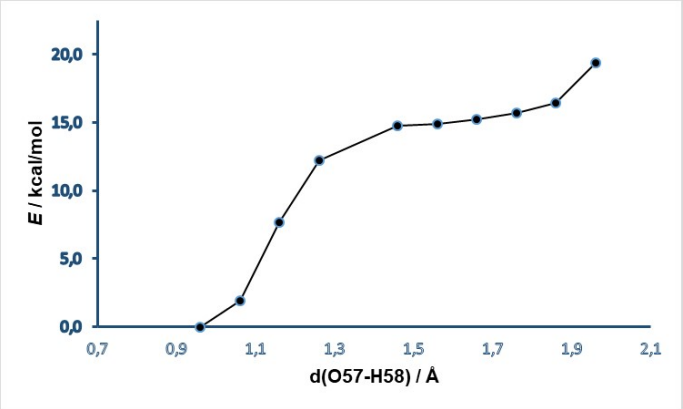

Figure S39. Potential energy scan (PES) of the reaction coordinate O57-H58 of the reaction of **C*** (+ $(TMS)_2NH$) to **5a** (+ $(TMS)_2N^-$).